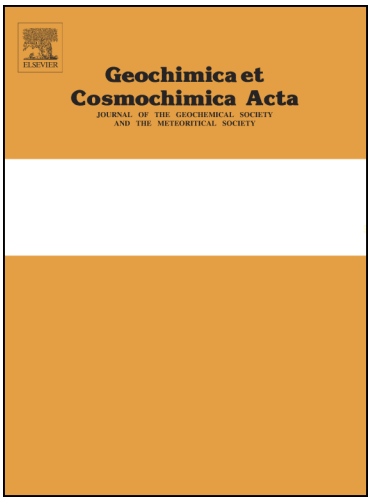

Records of Carbon and Sulfur Cycling During the Silurian Ireviken Event in Gotland, Sweden

Catherine V. Rose, Woodward W. Fischer, Seth Finnegan, David A. Fike

PII: S0016-7037(18)30660-4
DOI: https://doi.org/10.1016/j.gca.2018.11.030
Reference: GCA 11025

To appear in: *Geochimica et Cosmochimica Acta*

Received Date: 4 September 2018
Revised Date: 15 November 2018
Accepted Date: 21 November 2018

Please cite this article as: Rose, C.V., Fischer, W.W., Finnegan, S., Fike, D.A., Records of Carbon and Sulfur Cycling During the Silurian Ireviken Event in Gotland, Sweden, *Geochimica et Cosmochimica Acta* (2018), doi: https://doi.org/10.1016/j.gca.2018.11.030

Records of Carbon and Sulfur Cycling During the Silurian Ireviken Event in Gotland, Sweden

Catherine V. Rose[1*], Woodward W. Fischer[2], Seth Finnegan[3], & David A. Fike[4*]

[1]School of Earth & Environmental Sciences, University of St Andrews, Fife, KY16 9AL, UK;
[2]Division of Geological & Planetary Sciences, California Institute of Technology, Pasadena, CA 91125 USA;
[3]Department of Integrative Biology, University of California, Berkeley, CA 94720-3140 USA;
[4]Department of Earth & Planetary Sciences, Washington University, St. Louis, MO 63130 USA.

[*]Corresponding authors:
E-mail: cvr@st-andrews.ac.uk Phone: +44 01334 4632874
E-mail: dfike@levee.wustl.edu Phone: +1 (314) 935-6607

Abstract

Early Silurian (~431 Ma) carbonate rocks record a *ca*. 4.5‰ positive excursion in the stable isotopic composition of carbonate carbon ($\delta^{13}C_{carb}$). Associated with this isotopic shift is a macroevolutionary turnover pulse known as the 'Ireviken Event'. The onset of this carbon isotope excursion is commonly associated with a shallowing-upward facies transition that may have been accompanied by climatic change, as indicated by a parallel positive shift (~0.6‰) in the stable isotopic composition of carbonate oxygen ($\delta^{18}O_{carb}$). However, the relationships among carbon cycle perturbations, faunal turnover, and environmental changes remain enigmatic. Here we present a suite of new isotopic data across the Ireviken Event from multiple sections in Gotland, Sweden. These samples preserve no systematic change in $\delta^{18}O_{carb}$ but show positive excursions of equal magnitude in both carbonate ($\delta^{13}C_{carb}$) and organic ($\delta^{13}C_{org}$) carbon. In addition, the data reveal a synchronous perturbation in sulfur isotope ratios, manifest as a *ca*. 7‰ positive excursion in carbonate-associated sulfate ($\delta^{34}S_{CAS}$) and a *ca*. 30‰ positive excursion in pyrite ($\delta^{34}S_{pyr}$). The increase in $\delta^{34}S_{pyr}$ values is accompanied by a substantial, concomitant increase in stratigraphic variability of $\delta^{34}S_{pyr}$.

The relatively constant offset between the $\delta^{13}C_{carb}$ and $\delta^{13}C_{org}$ excursions throughout the Ireviken Event could be attributed to increased organic carbon burial, or possibly a change in the isotopic composition of CO_2 sources from weathering. However, a positive correlation between carbonate abundance and $\delta^{13}C_{carb}$ suggests that local to regional changes in dissolved inorganic carbon (DIC) during the shallowing-upward sequence may have been at least partly responsible for the observed excursion. The positive excursion recorded in $\delta^{34}S_{CAS}$ suggests a perturbation of sufficient magnitude and duration to have impacted the marine sulfate reservoir. An inverse correlation between CAS abundance and $\delta^{34}S_{CAS}$ supports the notion of decreased sulfate concentrations, at least locally, consistent with a concomitant increase in pyrite burial. A decrease in the offset between $\delta^{34}S_{CAS}$ and $\delta^{34}S_{pyr}$ values during the Ireviken Event suggests a substantial reduction in the isotopic fractionations (ε_{pyr}) expressed during microbial sulfur cycling and pyrite precipitation through this interval. Decreased ε_{pyr} and the concomitant increase in stratigraphic variation in $\delta^{34}S_{pyr}$ are typical of isotope systematics observed in modern shallow-water environments, associated with increased closed-system behavior and/or oxidative sedimentary reworking during early sediment diagenesis. While the isotopic trends associated with the Ireviken Event have been observed in multiple locations around the globe, many sections display different magnitudes of isotopic change, and moreover, are typically associated with local facies changes. Due to the stratigraphic coherence of the carbon and sulfur isotopic and abundance records across the Ireviken Event, and their relationship to changes in local depositional environment, we surmise that these patterns more closely reflect biogeochemical processes related to deposition and lithification of sediment than global changes in carbon and sulfur burial fluxes.

1. INTRODUCTION

The global carbon and sulfur biogeochemical cycles encompass a suite of fundamental interactions between the biosphere and Earth surface environments. Our understanding of the temporal evolution of biogeochemical cycling is primarily based on inferences drawn from the stable isotopic composition of carbon- and sulfur-bearing phases preserved in sedimentary strata (Garrels & Lerman, 1984; Holser et al., 1988; Hayes, 1993; Canfield, 2001a; Berner, 2006). The carbon-bearing phases are sedimentary carbonate carbon and organic carbon, reflecting the oxidized and reduced sinks, respectively (Hayes et al., 1999; Saltzmann & Thomas, 2012). Sulfate salts are the major oxidized sink for the sulfur cycle and are found in the form of sedimentary sulfate evaporite minerals (Holser, 1977; Canfield, 2001a; Kampschulte & Strauss, 2004), barite (Paytan et al., 2004), or carbonate-associated sulfate (CAS) - sulfate bound in the carbonate mineral lattice (Burdett et al., 1989). The reduced sulfur sink comes predominantly from pyrite, as well as organic sulfur (Werne et al., 2003; Werne & Lyons, 2005; Raven et al., 2016). These isotope proxies are sensitive to changing pathways and rates of microbial metabolic activity (Canfield, 2001a; Hayes, 2001; Sim et al., 2001b; Leavitt et al., 2013), as well as the burial flux of metabolic products, including organic matter and pyrite, in addition to the burial of carbonates and sulfate minerals (Garrels & Lerman, 1984; Kump & Garrels, 1986).

Perturbations to carbon and sulfur cycling occur throughout the geologic record and are typically observed as positive and negative excursions in $\delta^{13}C$ and/or $\delta^{34}S$ proxies. The Paleozoic sedimentary record includes multiple positive excursions in $\delta^{13}C_{carb}$ (Saltzman & Thomas, 2012). These excursions are commonly attributed to transient increases in organic carbon burial (Saltzman, 2005; Gill et al., 2011; Sim et al., 2015), although changes in the isotopic composition of weathering products entering the ocean also have been invoked (Kump et al., 1999). Similarly, transient increases in $\delta^{34}S$ often have been attributed to increased pyrite burial (Gill et al., 2007; Gill et al., 2011; Sim et al., 2015), or less commonly to changes in marine inputs (Canfield, 2004; Fike & Grotzinger, 2008). Coupled measurements of carbon and sulfur cycling can provide added constraints on forcing mechanisms as a result of their differential behavior in terms of magnitude and response time to a particular forcing (Fike et al., 2006; Gill et al., 2007; McFadden et al., 2008; Li et al., 2010; Jones & Fike, 2013; Gill et al., 2011; Sim et al., 2015).

The Late Ordovician Hirnantian Stage provides a well-studied example of the connections between biogeochemical cycling (parallel positive excursions (~4‰) in $\delta^{13}C_{carb}$ and $\delta^{13}C_{org}$ (Young et al., 2010; Jones et al., 2011)), changing climate (glaciation and associated cooling (Finnegan et al., 2011)), and marine extinctions (Sheehan, 2001; Delabroye & Vecoli, 2010; Melchin et al., 2013). Associated with the Hirnantian $\delta^{13}C$ excursion, there is a well-documented, synchronous positive excursion in pyrite ($\delta^{34}S_{pyr}$), although the magnitude (~20‰) and pre-excursion values vary slightly between locations (Yan et al., 2009; Zhang et al., 2009; Gorjan et al., 2012; Hammarlund et al., 2012). Interestingly, however, there is no accompanying excursion in sulfate $\delta^{34}S_{CAS}$ in the Hirnantian strata that have been studied (Jones & Fike, 2013; Gill et al., 2014; Present et al., 2015). This differential behavior of $\delta^{34}S_{CAS}$ vs. $\delta^{34}S_{pyr}$ records provides constraints on the nature of biogeochemical changes during the Hirnantian stage, suggesting that the positive excursion in $\delta^{34}S_{pyr}$ results from a transient decrease in the isotopic fractionation (ε_{pyr}) expressed between sulfate and pyrite (Jones & Fike, 2013). A decrease in ε_{pyr} could reflect enhanced organic loading (or increased organic matter degradation to organic acids usable by sulfate reducers) driving faster rates of cell-specific sulfate reduction (Sim et al., 2011b; Leavitt et al., 2013) and/or enhanced closed-system behavior (Gomes & Hurtgen, 2015), such as might be driven by enhanced organic carbon loading or increased sedimentation rates (Claypool, 2004; Pasquier et al., 2017). Both processes may have occurred during the sea level lowstand during the Hirnantian glacial maximum (Finnegan et al., 2012), potentially as well as increased rates of sulfide oxidation (Fry et al., 1988). The hypothesis that these processes might together reflect the impact of sea level change on ε_{pyr} in local stratigraphic sections is supported by observations of the depth-dependence on $\delta^{34}S_{pyr}$ values in modern sediments (Aller et al., 2010) and across recent glacial-interglacial transitions, where large (up to 75‰) variations in $\delta^{34}S_{pyr}$ appear to be predominantly driven by variable sedimentation rates during glacial and interglacial periods (Pasquier et al., 2017).

Here we examine the relationship between biogeochemical cycling, extinction, and sedimentology during the slightly younger Silurian (Sheinwoodian, ~431 Ma) Ireviken Event (Munnecke et al., 2003; Calner, 2008). This event is associated with the extinction of approximately 80% of conodont species and the extirpation of more than 50% of trilobite species in the Gotland record (Jeppsson, 1997a); there were also associated extinctions among acritarchs, chitinozoans, corals, brachiopods, and graptolites (Munnecke et al., 2003; Cooper et al., 2013).

Faunal turnover has been suggested to occur in eight discrete steps (Jeppsson, 1997a), with the largest extinction pulse occurring at Datum 2, just at or immediately below the Sheinwoodian-Homerian boundary, and the second largest pulse occurring at Datum 4 (Jeppsson, 1997a; Munnecke et al., 2003). Previous reports identified a ~ 4‰ positive excursion in carbonate carbon isotopes ($\delta^{13}C_{carb}$) at the onset of Datum 4 that is coincident with a small (~0.6‰) increase in carbonate oxygen isotopes ($\delta^{18}O_{carb}$), which may be evidence of changing climate or local hydrology (Munnecke et al., 2003). A bentonite located at Datum 2 has been dated to 431.8 ± 0.7 Ma and the duration of the associated $\delta^{13}C_{carb}$ excursion has been estimated to be ~ 1 Myr (from 431.5-430.5 Ma; Cramer et al., 2012). The $\delta^{13}C_{carb}$ excursion, biotic turnover, and facies change associated with the Ireviken Event has been observed in multiple sections around the globe (Table 1; Fig. 1). In many locations, the Ireviken Event is associated with local facies change, particularly in Baltica and Arctic Canada, where it is coincident with a sea level regression, and in central USA, Great Britain and Tunisia, where it appears to coincide with a transgression (Table 1). Here, we apply paired isotopic analysis of carbon ($\delta^{13}C_{carb}$, $\delta^{13}C_{org}$), oxygen ($\delta^{18}O_{carb}$), and sulfur (sulfate $\delta^{34}S_{CAS}$ and pyrite $\delta^{34}S_{pyr}$) phases in samples collected from stratigraphic sections across Silurian-aged strata of Gotland, Sweden, to improve our understanding of the changes in records of biogeochemical cycling during this event and their potential association with biological turnover and environmental change.

2. GEOLOGICAL SETTING

The stratigraphic section exposed on the island of Gotland, Sweden spans the latest Llandovery through the Wenlock stages of the Early Silurian epoch (Fig. 2). Formation ages and correlations between outcrops are well constrained by conodont and graptolite biostratigraphy (Jeppsson et al. 2006). The section records shelf, carbonate platform and backreef lagoon sediments deposited on the margin of the Baltic basin, which was situated within 30° of the equator during Early Silurian time (Fig. 1; Torsvik et al., 1992).

The oldest exposed strata on Gotland are the Lower Visby Beds, which consist of marls interbedded with fine-grained wavy-bedded to nodular argillaceous limestones and likely were deposited below storm-wave base (Fig. 3a; Calner et al., 2004b) (see SOM for petrographic descriptions and thin section images for all formations; Fig. S1). Fossils, primarily

rhynchonelliform brachiopods and bryozoans, are common but not abundant (Samtleben et al., 1996; Calner et al., 2004a). The contact between Lower and Upper Visby beds is marked by a condensed bed containing abundant fossils of the solitary rugose coral *Phaulactis* that has been interpreted as a maximum flooding surface (Samtleben et al., 1996; Jeppsson, 1997a; Munnecke et al., 2003; Calner et al., 2004b; Jeppsson et al., 2006). Conodont biostratigraphy places the Lower Visby-Upper Visby contact slightly above the Sheinwoodian-Homerian boundary (Jeppsson et al., 2006). Following Munnecke et al. (2003), we used the *Phaulactis* bed as the datum for correlating sections (Fig. 4). The Upper Visby records a shallowing-upwards cycle, where carbonate content progressively increases, associated with a decreased occurrence of marl beds and the appearance of bioclastic limestones and reef mounds. Ripple marks indicate deposition above storm-wave base. Fossils are abundant in the Upper Visby Beds (Fig. 3b, c) (Samtleben et al., 1996; Calner et al., 2004a).

The overlying Högklint Formation (Fm) consists of algal and crinoidal limestones with some reef mounds and was deposited above storm-wave base (Fig. 3d; Riding & Watts, 1991; Samtleben et al., 1996; Watts & Riding, 2000). The contact between the Högklint Fm and the overlying Tofta Fm has been interpreted as a sequence boundary (Calner et al., 2004b). The Tofta Fm consists of oncoid-rich bedded limestones with abundant leperditicopid ostracods and likely represents a shallow, restricted setting, such as a back-reef lagoon (Fig. 3e; Riding & Watts, 1991; Samtleben et al., 1996). Above the Tofta Fm, the Hangvar Fm consists of a distinct reef mound at the base of the unit with interbedded marls and limestones upsection, suggesting a transition to a deeper-water setting (Calner et al., 2004a).

The youngest strata we sampled were from the Slite Fm, which transitions from limestone to interbedded marly limestones and marls, reflecting deposition in deeper water (Fig. 3f-h). Strata are fossiliferous throughout this formation (Calner et al., 2004a; Cummins et al., 2014). Slite Group strata were sampled in section G13 (Cementa quarry) and are reported relative to an arbitrary datum at the base of the section due to an unknown thickness of unsampled strata above the top of the underlying sections.

The strata exposed on Gotland are exceptionally well preserved for their age. There has been very little tectonic deformation and strata are nearly horizontal (Jeppsson, 1983; Calner et al., 2004a). Thermal alteration is minimal with conodont alteration index (CAI) values of ~1 indicating a maximum temperature of ~100 °C (Jeppsson, 1983; Wenzel et al., 2000). Clumped

isotope paleothermometry (Eiler, 2007) on Gotland brachiopods and rugose corals gives low to moderate temperatures (30-60˚C; Cummins et al., 2014). The combination of clumped isotope data with classical water-rock paleothermometry indicates that diagenetic recrystallization primarily occurred as a closed-system (i.e., rock-buffered) process (Cummins et al., 2014).

The main extinction pulses of the Ireviken Event occur just before and at the boundary separating the Lower and Upper Visby beds (Jeppsson, 1997a; Munnecke et al., 2003). This Lower - Upper Visby contact also marks the onset of a +4‰ $\delta^{13}C_{carb}$ excursion and a +0.6‰ positive shift to increased $\delta^{18}O_{carb}$ values previously reported (Munnecke et al., 2003) and is associated with a trend toward shallower water depositional facies that lasts throughout the duration of the $\delta^{13}C_{carb}$ excursion (Calner et al., 2004a). The coincidence of the faunal turnover, biogeochemical perturbations, and changing depositional environment provide a framework to investigate the relationships between environmental, ecological, and depositional factors. Many workers have invoked a glacial cause for the Ireviken Event (Azmy et al., 1998; Kaljo et al., 2003; Brand et al., 2006; Calner, 2008) based on the similarity between the isotopic signatures ($\delta^{13}C_{carb}$ and, to a lesser extent, $\delta^{18}O_{carb}$) with the Late Ordovician Hirnantian ice age. However, the connection between the Hirnantian glaciation and carbon isotope excursion remains controversial (Melchin et al., 2013; Zhou et al., 2015). Recent conodont phosphate $\delta^{18}O$ analyses also support cooling (and/or expanded ice volume) during Ireviken time (Trotter et al., 2016). Widespread glacial tillites in Brazil are thought to be of latest Llandovery or earliest Wenlock age, supporting the idea that a cooling climate could be an integral part of the Ireviken Event (Grahn & Caputo, 1992).

3. METHODS

We collected a large suite of carbonate samples from outcrop in conjunction with measuring stratigraphic sections across Gotland (Fig. 2). Hand samples were slabbed with a rock saw to remove weathered surfaces. Material for carbonate carbon and oxygen isotopic analysis was obtained by drilling 100 mg of carbonate powder from samples in the field and from each slab back in the laboratory with a carbide dental drill, targeting well-preserved primary textures in predominantly fine-grained micrites. An additional portion (40-80 g) of each rock sample was

crushed to a homogeneous powder in a Spex 8515 shatterbox with an alumina ceramic vessel for subsequent sulfate and sulfide extractions.

Approximately 30 g of powdered sample was used for each sulfate extraction, following a modified version of the procedure of Burdett et al. (1989). The powder was soaked in a 10% NaCl solution for 12 hr and then rinsed three times in deionized water. Gradual addition of 6N HCl dissolved the carbonate matrix and liberated carbonate-associated sulfate (CAS). Acid addition continued until no carbonate remained. The resulting solution was filtered from the insoluble residue via vacuum filtration in three steps, finishing with a 0.2 μm filter. Saturated barium chloride solution was added to the filtrate to precipitate barium sulfate, which was isolated by centrifugation and rinsed with deionized water. The resulting barium sulfate was dried overnight at 70 °C.

Acid insoluble residue was rinsed with deionized water and dried at 70 °C, weighed, and then homogenized for subsequent extraction of pyrite sulfur using a method modified from Burton et al. (2008). Residue was placed in an airtight reaction flask. Air in the flask was flushed with N_2 gas. An acidified chromium chloride solution was injected to the reaction vessel, allowing any pyrite in the residue to react to form hydrogen sulfide gas, which was carried by the N_2 stream into the $AgNO_3$ trap. The sulfide gas reacted with the silver nitrate solution to precipitate silver sulfide. The resulting silver sulfide was centrifuged, rinsed, and dried at 70 °C.

Carbonate carbon and oxygen isotope ratios were measured using ~100 μg of drilled carbonate powder that was reacted for 4 hr at 72 °C with an excess of 100% H_3PO_4 in He-flushed, sealed tubes. Evolved CO_2 was sampled with a Thermo Finnigan Gas Bench II, and isotopic ratios were measured with a Thermo Finnigan Delta V Advantage gas source mass spectrometer at Washington University in St Louis (WUSTL). Isotopic measurements were calibrated against NBS-19, NBS-20, and two in-house standards, with analytical errors of < 0.1‰ (1σ) for $\delta^{13}C_{carb}$ and < 0.2‰ (1σ) for $\delta^{18}O_{carb}$.

Organic carbon isotopes were measured by combusting tin cups containing acid-insoluble residue in a Costech ECS 4010 Elemental Analyzer at 1000 °C. The mass of insoluble residue combusted was varied for each sample to give a constant peak size for CO_2 for subsequent isotopic analysis on a Thermo Finnegan Delta V Plus mass spectrometer at WUSTL. Isotopic measurements were calibrated against NBS-21 graphite, IAEA-CH6 sucrose, and in-house

acetanilide standards. All samples were measured in duplicate with an average reproducibility of < 0.25‰ (1σ) and are reported in delta notation relative to the V-PDB scale.

Isotopic analysis of the resulting sulfate and sulfide phases was performed using a Costech ECS 4010 elemental analyzer coupled to a Thermo Finnigan Delta V Plus mass spectrometer at WUSTL. For each analysis, approximately 100 μg of S was loaded into a tin capsule and combusted at 1000 °C. Sulfate sample combustion was catalyzed by the addition of ~2 mg of vanadium pentoxide to the sample capsules. The evolved SO_2 gas was introduced to the mass spectrometer in a continuous flow mode. Sulfur isotope composition was calibrated against NBS-127, IAEA-S1, and IAEA148. Sulfur isotope values are reported in permil (‰) relative to the V-CDT (Vienna Canyon Diablo Troilite) scale. Based on replicate analyses across several days, reproducibility of sulfur isotope measurements was < 0.3‰ (1σ).

A subset of 82 carbonate samples were selected for minor element analyses (Mg, Fe, Sr and Mn) from sections G1, G4, G5, G6 and G7 (refer to SOM; Fig. S2). Approximately 5 mg of each sample were placed in a 15 milliliter (mL) Falcon centrifuge tube along with 5 mL of a buffered solution of anhydrous acetic acid and ammonium hydroxide (pH of 5) and allowed to react in a sonicator for 5 h. This style of dissolution is effective in dissolving carbonate phases (both limestone and dolomite), but does not leach less soluble sediment components, such as Fe–Mn oxides and clays (Tessier et al., 1979; Husson et al., 2015). The elements liberated during dissolution are assumed to be carbonate-bound. Each solution was then centrifuged at 2500 rpm for ten minutes. The upper 4 mL of supernatant, clear of any insoluble residue, was pipetted off into another Falcon tube. Elemental abundances of Mg, Sr, Fe and Mn were measured on a PerkinElmer Optima 7300DV inductively coupled plasma optical emission spectrometer (ICP-OES) at WUSTL.

4. RESULTS

Isotopic data were obtained from 11 sections on Gotland (Fig. 2), spanning strata from the Lower Visby Fm through the Upper Visby, Högklint, and Tofta Fms, and into the Hangvar Fm, as well as strata from the overlying Slite Group (Fig. 3). Where present, sections where aligned at the contact between the Lower and Upper Visby Fms. Other sections were aligned based on their stratigraphic occurrence and the presence of the Ireviken $\delta^{13}C$ excursion (Fig. 4). Geochemical

results from Slite Group strata were tied into the other sections using the isotope ratio data of Cramer et al. (2012).

4.1. $\delta^{13}C_{carb}/\delta^{18}O_{carb}$

Beginning a few meters below the Lower Visby-Upper Visby contact, there is a 4.5‰ increase in $\delta^{13}C_{carb}$ (from ~1‰ to ~5.5‰) through the Upper Visby Fm spanning ~14 m of stratigraphy (Fig. 4). This increase in $\delta^{13}C_{carb}$ is associated with an increase in the abundance of carbonate from 80% to 100% (Fig. 5 and Fig. S3 in SOM). Throughout the overlying Högklint, Tofta, and lowermost Hangvar Fms, $\delta^{13}C_{carb}$ values remain at this +5.5‰ plateau with a slight trend down to values of 5‰ in the Hangvar Fm (Fig. 4). Following a sampling gap, $\delta^{13}C_{carb}$ returns to a relatively invariant value of ~ -1‰ in the overlying Slite Group strata. The basal Slite strata may record the tail end of the Ireviken $\delta^{13}C_{carb}$ excursion, although additional sampling of intervening strata is needed to ascertain this. For the most part, $\delta^{18}O_{carb}$ values cluster tightly around ~ -5.2‰ with only a few points more ^{18}O-depleted (to -6 or -7‰). We observed no evidence of the positive excursion in $\delta^{18}O_{carb}$ (Fig. 4) observed by Munnecke et al. (2003), likely reflecting more variable inputs and greater diagenetic alteration of oxygen isotope ratios in the carbonate matrix compared to the brachiopod shells studied by Munnecke et al. (2003). In the overlying Slite Group strata, $\delta^{18}O$ values are invariant at ~ -5.5‰ and no obvious offset was observed relative to the underlying strata.

4.2. $\delta^{13}C_{org}$

As is often the case, the $\delta^{13}C_{org}$ data show higher stratigraphic variability relative to that seen in co-occurring $\delta^{13}C_{carb}$. Despite this characteristic scatter, there is a ~ 5‰ positive shift in $\delta^{13}C_{org}$, which appears to slightly lag the $\delta^{13}C_{carb}$ excursion, rising from ~ -28‰ in the Lower Visby Fm to ~ -23‰ in the Tofta Fm (Fig. 4). Similar to the $\delta^{13}C_{carb}$ record, the observed increase in $\delta^{13}C_{org}$ is associated with a change in the abundance of the phase: here, total organic carbon (TOC) decreases associated with the increase in $\delta^{13}C_{org}$ values (Fig. 5 and SOM). Samples from the upper portion of section G4 (Upper Visby – Högklint Fms) are ~1-2‰ lower in $\delta^{13}C_{org}$ than expected relative to both the offset from coeval $\delta^{13}C_{carb}$ values and the $\delta^{13}C_{org}$ record from other sections (Fig. 4), suggesting local ecological controls on the $\delta^{13}C_{org}$ signal. The onset of the

increase in $\delta^{13}C_{org}$ is coincident with a shallowing upward transition from interbedded fossiliferous micrite and grainstones to biohermal facies. Throughout the overlying Högklint, Tofta, and lowermost Hangvar Fms, $\delta^{13}C_{corg}$ values remain elevated between -26‰ and -23‰ (Fig. 4). In the overlying Slite Group strata, $\delta^{13}C_{org}$ compositions returned to a relatively invariant value of ~ -30‰ that tracks the $\delta^{13}C_{carb}$ signal.

4.3. $\delta^{34}S_{CAS}$

The $\delta^{34}S_{CAS}$ data are characterized by ~5‰ variability throughout the sampled interval (Fig. 4). Superimposed on this scatter, $\delta^{34}S_{CAS}$ increases smoothly from ~30‰ in the Lower Visby Fm to ~37‰ at the top of the Upper Visby Fm (Fig. 4). This increase in $\delta^{34}S_{CAS}$ values with stratigraphic height is associated with a decrease in the abundance of CAS in these samples (Fig. 5 and SOM). The $\delta^{34}S_{CAS}$ values remain at ~37‰ through the Högklint and Tofta Fms and into basal Hangvar strata (Fig. 4). The overlying Slite Group strata have $\delta^{34}S_{CAS}$ values between 25‰ and 34‰ with no clear stratigraphic trend and an average of 32‰ ± 2‰ (n = 20).

4.4. $\delta^{34}S_{pyr}$

In the strata of the Lower and Upper Visby Fms, $\delta^{34}S_{pyr}$ values are relatively invariant at ~ -15‰ with scatter of ~10‰ at any given stratigraphic level (Fig. 4). The $\delta^{34}S_{pyr}$ values increase in the Upper Visby Fm, tracking the increase in $\delta^{34}S_{CAS}$. There is an abrupt 25‰ increase in $\delta^{34}S_{pyr}$ values to ~ +15‰ that occurs at the transition into the bioherms of the basal Högklint Fm (Fig. 4, 6). This shift is associated with a dramatic increase in $\delta^{34}S_{pyr}$ variability with a range of values up to ~ 70‰ across the Tofta-Hangvar Fm transition (Fig. 4). The $\delta^{34}S_{pyr}$ data are characterized by high stratigraphic variability relative to that in $\delta^{34}S_{CAS}$ in the Lower Visby Fm through Tofta Fm strata. The trend to higher and more variable $\delta^{34}S_{pyr}$ values is also associated with a decrease in the abundance of pyrite in these samples (Fig. 5 and SOM). In the overlying Slite Group, $\delta^{34}S_{pyr}$ decreases to -20‰ and is characterized by minimal variance (σ = 1.4‰) as compared to both its behavior lower in the section and to that of the co-occurring Slite Group $\delta^{34}S_{CAS}$ data (Fig. 4).

4.5 Minor elements

The Sr concentration shows limited variability throughout the stratigraphy associated with the Ireviken event but there are stratigraphic shifts in the Mg, Fe and Mn concentrations (Fig. S2). Mg displays the largest degree of variability with concentrations increasing from 1502 ppm in the Lower Visby Fm to 5074 ppm at the contact with the Upper Visby Fm. Similarly, there is a sharp rise in Fe concentration from 184 ppm to 1479 ppm and a slight shift in Mn concentration from 266 ppm to 362 ppm, both occurring just below the contact between the Lower and Upper Visby Formation. This sedimentological contact is a maximum flooding surface just prior to onset of the $\delta^{13}C_{carb}$ anomaly (Fig. 4).

5. DISCUSSION

5.1. Carbon cycling

The positive excursions in both $\delta^{13}C_{carb}$ and $\delta^{13}C_{org}$ are of similar magnitude (~ 4.5 – 5‰) with the shift in $\delta^{13}C_{carb}$ beginning ~2 m below the Lower Visby-Upper Visby contact and the $\delta^{13}C_{org}$ excursion rising more gradually with a slight ~10 m lag behind $\delta^{13}C_{carb}$. The shift in $\delta^{13}C_{carb}$ is also coincident with the onset of increased Fe abundance and aligns with some of the main extinction pulses (datums 3 and 5) of the Ireviken Event, occurring just before and at the boundary separating the Lower and Upper Visby beds. In contrast, the $\delta^{13}C_{carb}$ and $\delta^{13}C_{org}$ records in the overlying Slite Group are stratigraphically invariant and are characterized by values ~ 2‰ lower than their pre-Ireviken baselines.

Parallel time-series behavior in both $\delta^{13}C_{carb}$ and $\delta^{13}C_{org}$ data suggests a perturbation to the isotopic composition of the ambient dissolved inorganic carbon (DIC) reservoir during the Ireviken Event, directly impacting $\delta^{13}C_{carb}$ and in turn being incorporated into the $\delta^{13}C_{org}$ signature through relatively invariant (albeit local) biological fractionation (gray line in Fig. 4b). During the Ireviken event, there is little change in the apparent biological fractionation ($\varepsilon \sim \delta^{13}C_{carb} - \delta^{13}C_{org}$), with the exception of a ~2‰ decrease in the bioherm strata marking the Upper Visby-Högklint transition in section G4 (Fig. 4). In contrast, during the Hirnantian excursion, there is a sustained change in ε in some sections (Young et al., 2010), although not in all (Jones et al., 2011), and evidence for changing microbial community composition (Rohrssen et al., 2013). The increased stratigraphic scatter in $\delta^{13}C_{org}$ values relative to the $\delta^{13}C_{carb}$ values in the

same strata may simply reflect inherent variability in the isotopic fractionations associated with different carbon fixation pathways, variation in growth rates and growth conditions, and amounts of subsequent heterotrophic reworking (Laws et al., 1995; Hayes, 2001).

If the estimated duration of the Ireviken Event is correct (*ca*. 1 Myr), then the trends observed in the C isotopic data (i.e., the prolonged plateau at +5.5‰) are inconsistent with a transient perturbation to the carbon cycle, but rather suggest (near) equilibration to a new steady state characterized by elevated $\delta^{13}C_{carb}$ and $\delta^{13}C_{org}$ during this time. Although strata recording the termination of the Ireviken Event were not accessible for sampling in this study, the stratigraphically invariant $\delta^{13}C_{carb}$ and $\delta^{13}C_{org}$ data in the overlying Slite Group strata suggest that the carbon cycle had entered new quasi-equilibrium conditions by this time. This state is characterized by lower $\delta^{13}C_{carb}$ and $\delta^{13}C_{org}$ values—each ~2‰ lower than initial pre-Ireviken states.

Three parameters are commonly invoked to explain isotopic trends in $\delta^{13}C$ data that are attributed to change in global carbon cycling (e.g., Kump & Arthur, 1999): (1) the isotopic composition of DIC entering the oceans ($\delta^{13}C_{in}$); (2) the burial of organic carbon relative to total carbon burial (f_{org}); and (3) the isotopic fractionation(s) expressed between organic matter and source DIC, globally integrated as a single parameter, ε. At steady state:

$$\delta^{13}C_{carb} = \delta^{13}C_{in} + f_{org} * \varepsilon \qquad [1]$$

If changes in ε are ruled out, the observed $\delta^{13}C$ behavior during the Ireviken Event could be explained by either changes in f_{org} or $\delta^{13}C_{in}$. Assuming a constant $\delta^{13}C_{in}$ of ~ -5‰ (Kump & Arthur, 1999), the observed $\delta^{13}C$ signals could arise from a sustained increase in f_{org} from ~0.21 to ~0.38 during deposition of the Upper Visby through Hangvar Fms, followed by a decrease in f_{org} (~0.14) in the Slite Group. Alternatively, assuming f_{org} = 0.25 (average for this time from Hayes et al. (1999)), the observed $\delta^{13}C$ signals could arise from a sustained increase in $\delta^{13}C_{in}$ from ~ -5‰ to ~0‰ during deposition of the Upper Visby through Hangvar Fms, followed by a return to lower $\delta^{13}C_{in}$ values (-7‰) during deposition of the Slite Group. In this scenario, $\delta^{13}C_{in}$ would be expected to (broadly) track sea-level, with increased values possibly indicating enhanced carbonate weathering associated with lowstand and exposure of carbonate-rich basins (Kump et al., 1999). It is also possible that both f_{org} and $\delta^{13}C_{in}$ varied during this interval, which

would require smaller changes in either parameter individually (every 1‰ change in $\delta^{13}C_{in}$ having the same impact as a change of 0.04 in f_{org}).

An alternative interpretation of these $\delta^{13}C$ data is that they are influenced by local and/or regional environmental conditions and not necessarily record a simple time-series history of the global carbon cycle during this event. As a modern example, the Clino and Undo cores in the Bahamas are our best analogue for shallow water carbon isotope gradients (Swart & Eberli, 2005). The $\delta^{13}C_{carb}$ patterns in the marginal platform deposits are produced through the admixture of aragonite-rich sediments, which have relatively positive $\delta^{13}C_{carb}$ values, with pelagic materials, which have lower $\delta^{13}C_{carb}$ values (Swart & Eberli, 2005). As the more isotopically positive shallow-water carbonate sediments are only produced when the platforms are flooded, there is a connection between changes in global sea level and the $\delta^{13}C_{carb}$ of sediments in marginal settings. These data indicate that globally synchronous changes in $\delta^{13}C_{carb}$ can take place that are completely unrelated to, or caused by, variations in the global average burial of organic carbon. Thus, the $\delta^{13}C_{carb}$ values of the periplatform sediments in the Bahamas are largely unrelated to synchronous changes in the $\delta^{13}C_{carb}$ of the open-oceans observed over the same time period.

Two observations support the interpretation that the carbon data are influenced by local and/or regional environmental conditions. First, the onset (and termination) of the $\delta^{13}C$ excursion is associated with known changes in local depositional facies. Specifically, increased $\delta^{13}C_{carb}$ values are associated with the transition to shallow-water facies. Secondly, there is a strong correlation between the abundance of carbonate in a given sample and the measured $\delta^{13}C_{carb}$ signal. Specifically, the deeper water marls are ~80% carbonate and have lower $\delta^{13}C_{carb}$ values; whereas the shallower water facies, consisting of 95-100% carbonate are associated with the +5.5‰ $\delta^{13}C_{carb}$ plateau. The change in percent carbonate and depositional facies are best interpreted as local phenomena. Although it is possible to have global changes controlling these parameters (e.g., associated with eustatic sea level change during a glaciation, such as during the Hirnantian) (Opdyke & Walker, 1992; Swart & Eberli, 2005; Swart, 2008), the correlation of the $\delta^{13}C$ excursion with these local facies changes requires us to consider that the driving factor in the Ireviken $\delta^{13}C$ excursion could be a local and/or regional phenomenon. For example, the observed data could be explained by progressive changes in local DIC during the shallowing

upward sequence as the relative position of sediment deposition changes with respect to the $\delta^{13}C_{DIC}$ gradient arising from the biological pump (de La Rocha, 2003). Furthermore, the co-eval variability in Fe and Mn with Mg concentrations is broadly associated with the maximum flooding surface and the increased presence of micrite towards the Lower – Upper Visby Fm contact (Fig. S2). Micrite is expected to be less pristine than the brachiopod fragments or other fauna within the samples because it has high surface areas, far more commonly recrystallizes during burial, and often includes several generations of cements. Thus, this minor element variability might be associated with the facies transition from the progressively argillaceous beds and the flooding surface, as well as subsequent shallowing of the chemocline. To evaluate the relative support for these two distinctly different scenarios (global vs. local changes driving the $\delta^{13}C$ records), we turn to other proxy data.

5.2. Oxygen isotopes and climate

The $\delta^{18}O_{carb}$ record from well-preserved marine carbonate samples is sensitive to climate changes that could impact (i) ice-volume by changing seawater $\delta^{18}O$ (Shackleton & Opdyke, 1973), and/or (ii) ambient temperatures by changing the isotopic fractionation between seawater and carbonates (Emiliani & Edwards, 1953; Clayton, 1959). Local hydrologic changes, such as evaporation in partially restricted environments or influx of freshwater in estuarine settings, can additionally impact local $\delta^{18}O_{H2O}$ values and therefore $\delta^{18}O_{carb}$ values. In addition, changes in the relative contributions of aragonitic vs. calcitic carbonate producers (Lécuyer et al., 2012) and/or kinetic/'vital' effects could also impact the resulting $\delta^{18}O_{carb}$ values (Adkins et al., 2003). Previous reports have identified a +0.6‰ increase in $\delta^{18}O_{carb}$ from well-preserved brachiopods spanning the Ireviken Event, a signal that has been interpreted to reflect changes in local hydrography of the basin during deposition (Bickert et al., 1997; Munnecke et al., 2003).

We observed no corresponding stratigraphically coherent change in $\delta^{18}O_{carb}$ (Fig. 4), although our sampling was broad and unlike previous studies did not focus on well-preserved fossils. The absence of a $\delta^{18}O_{carb}$ excursion from our data likely indicates that the samples have undergone variable diagenetic alteration to mask the $\delta^{18}O_{carb}$ anomaly (without a corresponding impact on the $\delta^{13}C_{carb}$ signature, which is rock-buffered and hence more robust (Cummins et al., 2014)). In addition to the above results, clumped isotope paleothermometry (Eiler, 2007) was applied to well-preserved brachiopods from the same sample suite presented here. Although

dealing with limited samples, this work did not reveal evidence for a substantive change in either seawater $\delta^{18}O$ or temperature that would be expected to drive a primary change in $\delta^{18}O_{carb}$ during the Ireviken Event (Cummins et al., 2014). However, there is a record of increased $\delta^{18}O$ enrichment found in conodonts from many sections through the Ireviken (Trotter et al., 2016), which is similar in magnitude to the increase in $\delta^{18}O_{carb}$ found previously (Bickert et al., 1997; Munnecke et al., 2003). These phosphate ($\delta^{18}O_{PO4}$) records are thought to be more robust against diagenetic alteration than the records from carbonate phases (Wenzel & Joachimski, 1996) and may more accurately record primary changes in climate associated with either cooling and/or increase in ice volume during Ireviken time. Thus, while we saw no clear $\delta^{18}O_{carb}$ evidence for cooling or glaciation in our data, the preponderance of results from other studies is consistent with the hypothesis that climate change was linked to the Ireviken Event and associated with the observed changes in carbon and sulfur isotopic records.

5.3. Sulfur cycling

Changes in both $\delta^{34}S_{CAS}$ and $\delta^{34}S_{pyr}$ values were observed in unison with the $\delta^{13}C$ excursion. Unlike the carbon isotope excursions, the magnitudes of the trends are fundamentally different between sulfate and sulfide: $\delta^{34}S_{CAS}$ increases by 7‰, whereas the observed increase in $\delta^{34}S_{pyr}$ is roughly four times as large (~30‰; Fig. 4). Stratigraphic variability (i.e., the range of $\delta^{34}S$ in each facies at any particular stratigraphic position) in $\delta^{34}S_{CAS}$ is roughly constant (~5‰) throughout the stratigraphy. In contrast, variability of $\delta^{34}S_{pyr}$ increases upsection from 7.4‰ (1σ) in the Lower/Upper Visby strata, to 8.5‰ (1σ) in the Högklint Fm, to as high as 16.6‰ (1σ) in the Tofta-Hangvar strata, before ultimately decreasing to 1.4‰ (1σ) in the overlying Slite Group (Fig. 4).

Akin to the relationship between $\delta^{13}C_{carb}$ and $\delta^{13}C_{org}$, $\delta^{34}S_{pyr}$ is expected to show larger scatter than $\delta^{34}S_{CAS}$ because of variable isotopic fractionation during microbial sulfur cycling likely occuring in the sediment column during early diagenesis (Fry et al., 1988; Canfield & Teske, 1996; Habicht et al., 1998; Canfield, 2001b; Fike et al., 2008; Sim et al., 2001b; Fike et al., 2015). In contrast to $\delta^{13}C_{org}$ values, there can be additional variability in the $\delta^{34}S_{pyr}$ signal associated with possible closed-system distillation for pyrites forming in the sediment under limited porewater exchange with the overlying water column (Gomes & Hurtgen, 2013). Thus,

the apparent fractionation observed between $\delta^{34}S_{CAS}$ and $\delta^{34}S_{pyr}$ records can reflect both biological and sedimentological factors (Pasquier et al., 2017).

Variability in $\delta^{34}S_{CAS}$ (σ = 3.0‰) is less than $\delta^{34}S_{pyr}$ (σ = 14.7‰) variability in the lower portions of the stratigraphy (Lower Visby through Hangvar Fms), but much higher than $\delta^{34}S_{pyr}$ variability in the Slite Group strata (Fig. 4). Slite Group strata have higher variability in $\delta^{34}S_{CAS}$ (σ = 2.1‰) than in $\delta^{34}S_{pyr}$ (σ = 1.4‰), which is unexpected from coeval sulfur phases and suggests (1) multiple, geochemically distinct carbonate phases (Present et al., 2015); (2) possible alteration of $\delta^{34}S_{CAS}$ after deposition and/or during processing (Wotte et al., 2012); or (3) potential overprinting of $\delta^{34}S_{pyr}$ values due to post-depositional migration of sulfur-bearing fluids. We observed no evidence of macroscopic sulfide phases such as pyrite within the Slite Group or clear indication of diagenetic fluid migration to support the last scenario (Fig. S1; refer to SOM). If primary, the stability of $\delta^{34}S_{pyr}$ in Slite strata argues for similar stability in both the parent $\delta^{34}S_{SO4}$ and in the apparent fractionation ε (arising from the combined effects of the actual biological metabolisms and any subsequent closed-system distillation). Consequently, we view the observed variation in $\delta^{34}S_{CAS}$ as more likely the result of carbonate precipitation in porewaters that had become chemically distinct from overlying seawater (e.g., as the result of progressive sulfate reduction) or from interaction with later-stage fluids with a distinct sulfate composition (Marenco et al., 2008a; Marenco et al., 2008b; Jones & Fike, 2013; Present et al., 2015). This interpretation is consistent with the nodular nature of these beds in many locations, evidence for discrete but variable precipitation of carbonate on the seafloor and within the sediment column. Additional variability in the $\delta^{34}S_{CAS}$ data could arise from incomplete removal of secondary sulfates (Wotte et al. 2012) not truly bound into the carbonate mineral lattice, such as those derived from atmospheric deposition (Peng et al., 2014) or in-situ oxidation of sulfides over geologic time.

Standard isotope mass balance models of global sulfur cycling treat stratigraphic sulfur isotope variation in terms of three parameters (Canfield, 2004; Fike & Grotzinger, 2008): (1) the isotopic composition of sulfate entering the oceans ($\delta^{34}S_{in}$); (2) the relative burial of pyrite sulfur compared to total sulfur burial (f_{pyr}); and (3) the expressed isotopic fractionation between sulfate and hydrogen sulfide, which is approximated by the isotopic offset between sulfate and pyrite in ancient strata: ε_{pyr}. At steady state:

$$\delta^{34}S_{CAS} = \delta^{34}S_{in} + f_{pyr} * \varepsilon_{pyr} \quad [2]$$

The first-order increases in both $\delta^{34}S_{CAS}$ and $\delta^{34}S_{pyr}$ values across the Ireviken Event naturally suggest the hypothesis that both reflect a remarkably rapid change to the isotopic composition of the local sulfate reservoir. This sulfate reservoir is the source of sulfur incorporated into carbonates as $\delta^{34}S_{CAS}$ and into pyrites following microbial sulfate reduction to hydrogen sulfide and subsequent reaction with iron (Berner, 1984). All else being equal, a change in the isotopic composition of the marine sulfate reservoir ($\delta^{34}S_{SO4}$) would be inherited by pyrites formed from this parent sulfate. Thus, we can divide the observed $\delta^{34}S$ response into two components: (1) a +7‰ positive excursion in both sulfate and pyrite $\delta^{34}S$; and (2) an additional factor driving the further ~23‰ increase in mean $\delta^{34}S_{pyr}$ and associated increase in $\delta^{34}S_{pyr}$ variability.

If these S isotopic data reflect changes in the global sulfur cycle, the parallel increase in $\delta^{34}S_{CAS}$ and $\delta^{34}S_{pyr}$ can be explained by either changes in f_{pyr} or $\delta^{34}S_{in}$ [Eq 2]. Isotopic mass-balance arguments (Canfield, 2004; Fike & Grotzinger, 2008) require early Paleozoic $\delta^{34}S_{in}$ to be significantly more enriched than bulk Earth (0‰) or estimates of average modern marine inputs (~3‰) (Canfield, 2004; Burke et al., 2015). However, no firm estimates exist for $\delta^{34}S_{in}$ during Silurian time. As such, we can only discuss relative changes in both $\delta^{34}S_{in}$ and f_{pyr}. The generation of a 7‰ parallel increase in sulfate and pyrite $\delta^{34}S$ could be accomplished by a 7‰ increase in $\delta^{34}S_{in}$ or an increase in f_{pyr} of ~ 0.23 (assuming an average ε_{pyr} of 30‰ (Wu et al., 2010)). It is also possible that both f_{pyr} and $\delta^{34}S_{in}$ varied during this interval, which would require correspondingly smaller changes in either parameter individually (every 3‰ change in $\delta^{34}S_{in}$ having the same impact as a 0.1 change in f_{pyr}).

An alternative view of the $\delta^{34}S_{CAS}$ data is that they reflect changes that occurred in a local sulfate pool, rather than the global marine sulfate reservoir. This interpretation is supported by three observations. First, the onset (and termination) of the excursion is associated with changes in local depositional facies; $\delta^{34}S_{CAS}$ values increase during the transition to shallow water facies. Second, there is an inverse correlation between CAS abundance (ppm) and the measured $\delta^{34}S_{CAS}$ values (Figure 5; SOM). This relationship is consistent with partial closed-system distillation of the reservoir in the shallower, more restricted facies, resulting in decreased sulfate abundance and increased $\delta^{34}S_{SO4}$. While this scenario could apply to the entire ocean rather than the local sulfate pool, the short duration of this event (~1 million years) suggests that such a large change in marine sulfate concentrations is unlikely. Such a change would also be unlikely to happen in

lockstep with local facies changes. Third, the upper strata of the Slite Group locally record pseudomorphs after gypsum atop patch reefs, thought to have been precipitated during a transient regression (Faerber & Munnecke, 2014). This observation requires that marine sulfate levels were sufficiently high during this interval to ensure gypsum precipitation before halite saturation (e.g., > ~3mM). These sulfate levels appear to be too high to readily accommodate an isotopic change of the observed magnitude in the global seawater sulfate reservoir over the duration of the Ireviken (Luo et al., 2010). The scatter of the $\delta^{34}S_{CAS}$ record (± ~5‰) is also larger than would be expected if it faithfully reflected the global seawater reservoir because the amount of time allowable is insufficient for the oceanic reservoir to change so substantially on such short time scales. What then might explain this variation in $\delta^{34}S_{CAS}$?

One possibility is late diagenetic alteration. However, the excellent preservation of these strata and general absence of evidence for significant diagenetic alteration (Jeppsson, 1983; Wenzel et al., 2000; Calner et al., 2004a; Cummins et al., 2014), suggests that a wholesale overprinting of the $\delta^{34}S_{CAS}$ record is unlikely. In these strata, carbonates generally formed in the water column or at or near the sediment-water interface, and can reasonably be inferred to reflect ambient seawater and shallow porewater chemistry at the time of deposition, modified by early diagenetic cements associated with lithification. The addition of late phase carbonate cements (including those associated with meteoric and/or basinal diagenesis), with their own sulfate concentrations and respective isotopic compositions, could variably overprint the original seawater signature, shifting values and/or increasing scatter in the $\delta^{34}S_{CAS}$ record. Such variability was observed in the Hirnantian-aged strata from Anticosti Island, both in bulk-rock values (Jones & Fike, 2013) and when sampled at the mm-scale (Present et al., 2015). The increased stratigraphic variation in $\delta^{34}S_{CAS}$ values relative to $\delta^{34}S_{pyr}$ values in Slite Group strata does suggest a modest degree (± ~3‰) of local alteration to the $\delta^{34}S_{CAS}$ record, at least in this interval (Fig. 4). More explicitly, if the relatively invariant $\delta^{34}S_{pyr}$ signal is primary, it requires that the alteration to the $\delta^{34}S_{CAS}$ values happen after in-situ pyrite formation (i.e., the $\delta^{34}S_{CAS}$ variability cannot reflect perturbations to the local water column $\delta^{34}S_{SO4}$). These observations lead us to consider that the driving factor(s) in the Ireviken $\delta^{34}S_{CAS}$ excursion may be at least in part a local phenomenon.

Superimposed on this parallel 7‰ increase in $\delta^{34}S_{CAS}$ and $\delta^{34}S_{pyr}$, additional factors are needed to explain the further ~23‰ increase in $\delta^{34}S_{pyr}$ and concomitant substantial increase in $\delta^{34}S_{pyr}$ variability. Examining paired $\delta^{34}S_{CAS}$ and $\delta^{34}S_{pyr}$ data, it is clear that there are stratigraphically coherent changes in both the magnitude and variability of ε_{pyr} preserved. Specifically, in the Lower Visby Fm, ε_{pyr} is ~45‰ with moderate variability (σ = 9.7‰), decreasing to an average of ~20‰ with very large variability (from ~ -10 to +55‰; σ = 15.1‰) in the Upper Visby through Hangvar Fms, and increasing to ε_{pyr} ~ 52‰ with minimal variability (σ = 1.4‰) in the overlying Slite Group. The differential magnitude of the increases in $\delta^{34}S_{CAS}$ and $\delta^{34}S_{pyr}$ during the Ireviken Event imply considerable changes in the expressed isotopic fractionation ($\varepsilon_{pyr} = \delta^{34}S_{CAS} - \delta^{34}S_{pyr}$) during sulfur cycling at this time. The covariation with lithofacies hints toward explanations for the decrease in ε_{pyr} and associated increase its variability that invoke changes occuring in the depositional environment. Environmental changes can impact ε_{pyr} (Claypool, 2004; Gomes & Hurtgen, 2013; Pasquier et al., 2017), particularly when the sites of sulfate incorporation (carbonate precipitation) and sulfide / pyrite formation are separated in space or time (Fike et al., 2015).

Even more so than fractionations associated with carbon fixation, isotopic fractionations during microbial sulfur cycling can be large and extremely variable (between 0‰ and 70‰), depending on a variety of ecological and environmental factors (Fry et al., 1988; Canfield & Teske, 1996; Habicht et al., 1998; Canfield, 2001b; Habicht et al., 2002; Claypool, 2004; Fike et al., 2009; Sim et al., 2011b; Leavitt et al., 2013). In terms of strictly biological causes, a change in the relative abundance/activity of various sulfur cycling metabolisms (e.g., sulfate reduction, sulfur disproportionation, sulfide oxidation), each with their own isotopic fractionations, can impact the net fractionation between sulfate and sulfide. Sulfate reduction is generally thought to have the largest impact on overall isotopic fractionation in marine systems. Fractionation during sulfate reduction is mediated primarily by variations in the cell-specific rates of sulfate reduction, driven by the types and availability of electron donors coupled to sulfate reduction (Sim et al., 2011a; Sim et al., 2011b; Leavitt et al., 2013). One scenario to explain the decreased ε_{pyr} values observed during the Ireviken Event (Fig. 4) would be as the result of increased sedimentary organic carbon loading that drove faster rates of sulfate reduction, for a given sediment flux. Alternatively, changes in sedimentation rate could impact the connectivity of pore

waters to the overlying water column (Pasquier et al., 2017; Claypool, 2004). Increased sedimentation would isolate the local pore water sulfate reservoir, leading to increased pore water $\delta^{34}S_{SO4}$ through ongoing microbial sulfate reduction. Conversely, slower sedimentation rates and higher porosity would result in enhanced communication between pore water and seawater. In this relatively open system, the constant supply of seawater sulfate results in a stable, low value for pore water $\delta^{34}S_{SO4}$ (and therefore in the resulting $\delta^{34}S_{pyr}$) in these intervals. Decreased ε_{pyr} could also result from increased sulfide oxidation in shallower, more energetic environments, which could drive the residual sulfide pool to increased $\delta^{34}S_{H2S}$ values (Fry et al., 1988) and/or impact the availability of reactive iron that can react with H_2S to eventually form pyrite. Given the observed facies changes and decrease in TOC associated with the Ireviken Event in these samples, the latter options of changing sedimentation rates and/or more oxidizing conditions seem more likely than increased sulfate reduction rates and closed-system behavior resulting from enhanced organic carbon loading. Following reaction with iron, this enriched sulfide pool would create pyrites with elevated $\delta^{34}S_{pyr}$ (Fike et al., 2015), as observed (Fig. 4).

There is a strong case for a depositional influence of the $\delta^{34}S_{pyr}$ signature – over and above that acting on the (local) parent $\delta^{34}S_{SO4}$ reservoir. Specifically, a major increase in both average $\delta^{34}S_{pyr}$ and associated stratigraphic variability occurs abruptly at the Upper Visby-Högklint transition, coincident with the transition to shallow-water biohermal facies (e.g., Fig. 6). This shallowing represents a shift to a shallower, more energetic depositional environment. In modern ocean sediments, such a transition can lead to increases in both the mean value and the stratigraphic variation of $\delta^{34}S_{pyr}$ (e.g., Aller et al., 2010; Gao et al., 2013). Storm-induced sedimentary reworking juxtaposes newly re-deposited oxic sediments with underlying sulfide sediments.

Oxidative reworking has three potential consequences. First, partial oxidation of ambient H_2S along the reworked contact can result in an increase in residual $\delta^{34}S_{H2S}$ (Fry et al., 1988). Secondly, higher rates of cell-specific sulfate reduction (associated with the sharp redox gradient) can result in the generation of new hydrogen sulfide with decreased fractionation from its parent sulfate (Sim et al., 2011b; Wing & Halevy, 2014). Thirdly, the presence of the oxidized layer encourages the partial isolation of the zone of net sulfate reduction at the base of the reworked layer from the overlying seawater boundary, leading to closed-system behavior

with the generation of ^{34}S-enriched sulfate and, in turn, ^{34}S-enriched sulfide following progressive sulfate reduction.

Thus, the changing depositional environment associated with the shallowing-upward transition from Upper Visby through Hangvar Fms might explain both the increase in $\delta^{34}S_{pyr}$ beyond that found in coeval $\delta^{34}S_{CAS}$ and also the increase in stratigraphic variability in $\delta^{34}S_{pyr}$. A dependence of both mean ε_{pyr} and its variance on depositional environment is supported by the abrupt changes in these parameters at the Upper Visby-Högklint boundary, coincident with the transition to shallow water bioherm facies representative of a more energetic depositional environment (Fig. 6). In addition, bioturbation and its potential impact on both biogeochemical cycling and the signals that get preserved in sediments is important. Whilst bioturbation is present within some of the sediments as marked by nodular bedding and vertical traces, the degrees of bioturbation within the Silurian are far lower than seen in Mesozoic or Cenozoic environments (Tarhan et al., 2015).

5.4. Global importance

Given the inferred environmental influence on the proxies examined here ($\delta^{13}C_{carb}$, $\delta^{13}C_{org}$, $\delta^{34}S_{CAS}$, and especially $\delta^{34}S_{pyr}$), the stratigraphic records through the Ireviken Event observed here would not necessarily be expected to be globally reproducible, in contrast to the standard interpretation of these proxies, particularly $\delta^{13}C_{carb}$ and $\delta^{34}S_{CAS,}$ which are often thought to reflect global marine reservoirs. However, there are records from around the world demonstrating the presence of both the Ireviken Event extinction and the associated $\delta^{13}C$ excursion (Table 1). How do we reconcile these? In examining the global records of Ireviken $\delta^{13}C$ data, two patterns are clear: first, the magnitude of the excursion varies strongly from location to location (from ~2-5.5‰); and secondly, most of these instances are coincident with clearly recognized facies transitions (Table 1).

These observations could be reconciled if there were global processes that synchronously gave rise to local facies changes and variable biogeochemical changes in basins around the world. Based on the timing of the Ireviken Event, the most obvious candidate for a driving mechanism would be a pulse of cooling (possibly associated with glaciation) coincident with the Ireviken. This hypothesis is consistent with the $\delta^{18}O_{carb}$ (Bickert et al., 1997; Munnecke et al., 2003) and conodont phosphate ($\delta^{18}O_{PO4}$) records (Trotter et al., 2016) and potentially the

sedimentary record (Grahn & Caputo, 1992), although as discussed above no evidence for this was found using carbonate clumped isotopes on a subset of Gotland samples (Cummins et al., 2014). In this framework, cooling-induced seawater contraction and associated sea level drop (plus possible glacioeustatic sea-level change) could influence depositional settings across the globe, impacting in turn how local conditions filter the ways in which biogeochemical proxies get encoded in sediments. These interpretations are fundamentally in agreement with Jeppsson's original model that invokes climatically driven changes in local hydrology to explain the Ireviken Event as a function of alternating humid/arid episodes (Jeppsson, 1990; Bickert et al., 1997; Jeppsson, 1997a; Munnecke et al., 2003). The results here add to the growing appreciation that chemostratigraphic isotopic records, particularly $\delta^{34}S_{pyr}$, can be impacted by both local and global processes. It is also important to note that despite occurrences where changes in local depositional settings around the world might be synchronous, the expressed isotopic excursions themselves might not be of global significance from an isotope mass-balance perspective. For example, local changes in deposition could result in extra organic matter burial in shallow environments throughout the world, resulting in a global increase in $\delta^{13}C_{carb}$ mediated through global $\delta^{13}C_{DIC}$. However, if sea level changes create a number of Bahamas-like carbonate platforms, it is possible that an associated increase in local $\delta^{13}C_{carb}$ signatures in these sections would have no global significance from an isotope mass balance perspective (Swart, 2008; Swart & Eberli, 2005). If such environments of local ^{13}C-enriched carbonate deposition are sufficiently widespread as to become a major global carbonate sink, they will perforce induce a decrease in $\delta^{13}C$ in the average surface ocean to maintain mass balance.

The recognition that chemostratigraphic isotopic records, particularly $\delta^{34}S_{pyr}$, can be impacted by both local and global processes demands consideration when making inferences about changes in global biogeochemical cycling based on local geochemical records, particularly when they change in sync with local depositional facies. Furthermore, many geochemical proxies record both global *and* local processes. Therefore, paired sedimentological and chemostratigraphic data are essential to tease these signals apart for accurate interpretation of proxy data in the rock record.

6. CONCLUSIONS

Carbonate rocks from the early Silurian (Sheinwoodian, ~431 Ma) contain a record of a substantial extinction of marine taxa known as the Ireviken Event. On Gotland, these rocks record positive excursions of approximately equal magnitude in both carbonate ($\delta^{13}C_{carb}$) and organic ($\delta^{13}C_{org}$) carbon, as well as a synchronous perturbation to the sulfur cycle manifest as an ~7‰ positive excursion in $\delta^{34}S_{CAS}$ and an ~30‰ positive excursion in $\delta^{34}S_{pyr}$. The additional increase in $\delta^{34}S_{pyr}$ values is accompanied by a concomitant increase in stratigraphic variability of $\delta^{34}S_{pyr}$ values, both of which are potentially attributable to a transition to shallower, higher-energy conditions (Aller et al., 2010; Pasquier et al., 2017). All of these proxy records show relationships between the abundance of a given phase and its isotopic composition—and these changes also co-occur with changes in lithofacies and paleoenvironmental conditions. However, the Ireviken Event (both the biotic turnover and the $\delta^{13}C$ excursion) appears in stratigraphic sections around the world, where the stratigraphic trends are also frequently associated with changing depositional facies, perhaps related to glacioeustatic sea-level changes. Because these chemostratigraphic isotopic records, particularly $\delta^{34}S_{pyr}$, can be impacted by both local *and* global processes, paired sedimentological and chemostratigraphic data are essential to tease these signatures apart and more accurately reconstruct biogeochemical cycling over Earth history. These observations require revisions in how we apply stable isotope proxies to reconstruct historical carbon and sulfur budgets. While this uncertainty may be discouraging to some, recognition of this complexity provides new geochemical opportunities to interrogate conditions of depositional facies and diagenetic regimes.

Acknowledgments – Field and stable isotope work was supported by an Agouron Institute grant to DAF and WWF as well as a Packard Fellowship and a Hanse-wissenschaftskolleg Fellowship awarded to DAF. J. G. Metzger assisted with field work. S. Moore and C. Beaudoin helped with sample preparation and S. Moore and D. McCay assisted with stable isotope measurements at Washington University in St. Louis. Reviews by Lee Kump, Matt Hurtgen, and Noah Planavsky improved this manuscript.

APPENDIX A. SUPPLEMENTARY DATA

Data presented in this article can be found in supplementary spreadsheet and Table S1.

REFERENCES

Adkins, J.F., Boyle, E.A., Curry, W.B., Lutringer, A., 2003. Stable isotopes in deep-sea corals and a new mechanism for "vital effects". Geochimica Et Cosmochimica Acta, 67(6): 1129-1143.

Aller, R.C., Madrid, V., Chistoserdov, A., Aller, J.Y., Heilbrun, C., 2010. Unsteady diagenetic processes and sulfur biogeochemistry in tropical deltaic muds: Implications for oceanic isotope cycles and the sedimentary record. Geochimica et Cosmochimica Acta, 74: 4671 - 4692.

Azmy, K., Veizer, J., Bassett, M., Copper, P., 1998. Oxygen and carbon isotopic composition of Silurian brachiopods: implications for coeval seawater and glaciations. Geol. Soc. Am. Bull., 110: 1499–1512.

Berner, R.A., 1984. Sedimentary pyrite formation: an update. Geochimica et Cosmochimica Acta, 48: 605 - 615.

Berner, R.A., 2006. GEOCARBSULF: A combined model for Phanerozoic atmospheric O2 and CO2. Geochimica et Cosmochimica Acta, 70(23): 5653 - 5664.

Bickert, T., Pätzold, J., Samtleben, C., Munnecke, A., 1997. Paleoenvironmental changes in the Silurian indicated by stable isotopes in brachiopod shells from Gotland, Sweden. Geochim. et Cosmochim. Acta, 61: 2717 - 2730.

Brand, U., Azmy, K., Veizer, J., 2006. Evaluation of the Salinic I tectonic, Cancañiri glacial and Ireviken biotic events: Biochemostratigraphy of the Lower Silurian succession in the Niagara Gorge area, Canada and U.S.A. Palaeogeography Palaeoclimatolofy Palaeoecology, 241: 192–213.

Burdett, J.W., Arthur, M.A., Richardson, M., 1989. A Neogene seawater sulfate isotope age curve from calcareous pelagic microfossils. Earth and Planetary Science Letters, 94(3-4): 189-198.

Burke, A., Adkins, J., Gaillardet, J., Paris, G., Peucker-Ehrenbrink, B., Voss, B., Spencer, R., Holmes, R.M., McClelland, J., 2015. Isotopic Constraints on Riverine Sulfur Sources: A Global Perspective, Goldschmidt Abstracts, pp. 427.

Burton, E.D., Sullivan, L.A., Bush, R.T., Johnston, S.G., Keene, A.F., 2008. A simple and inexpensive chromium-reducible sulfur method for acid-sulfate soils. Applied Geochemistry, 23: 2759 - 2766.

Calner, M., 2008. Silurian global events – at the tipping point of climate change. In: Elewa, A.M.T. (Editor), Mass extinctions. Springer-Verlag, Berlin & Heidelberg, pp. 21 - 58.

Calner, M., Jeppsson, L., Munnecke, A., 2004a. Field Guide to the Silurian of Gotland - Part I. Erlanger Geol. Abh., 5: 113–131.

Calner, M., Jeppsson, L., Munnecke, A., 2004b. Field Guide to the Silurian of Gotland - Part II. Erlanger Geol. Abh., 5: 133 - 151.

Canfield, D.E., 2001a. Biogeochemistry of sulfur isotopes. Reviews in Mineralogy & Geochemistry: Stable Isotope Geochemistry, 43: 607-636.

Canfield, D.E., 2001b. Isotope fractionation by natural populations of sulfate-reducing bacteria. Geochimica et Cosmochimica Acta, 65: 1117 - 1124.

Canfield, D.E., 2004. The evolution of the Earth surface sulfur reservoir. American Journal of Science, 304(10): 839-861.

Canfield, D.E., Teske, A., 1996. Late Proterozoic rise in atmospheric oxygen concentration inferred from phylogenetic and sulphur-isotope studies. Nature, 382(6587): 127-132.

Claypool, G.E., 2004. Ventilation of marine sediments indicated by depth profiles of pore water sulfate and $\delta^{34}S$. Special Publication, Geochemical Society, 9: 59 - 65.

Clayton, R.N., 1959. Oxygen isotope fractionation in the system calcium carbonate - water. Journal of Chemical Physics, 30(5): 1346 - 1350.

Cocks, L.R.M., Torsvik, T.H., 2002. Earth Geography from 500 to 400 million years ago: a faunal and palaeomagnetic review. *Journal of the Geological Society, London*, 159, 631-644.

Cooper, R.A., Sadler, P.M., Munnecke, A., Crampton, J.S., 2013. Graptoloid evolutionary rates track Ordovician–Silurian global climate change. Geological Magazine, 151(2): 349 - 364.

Cramer, B.D., Condon, D.J., Söderlund, U., Marshall, C., Worton, G.J., Thomas, A.T., Calner, M., Ray, D.C., Perrier, V., Boomer, I., Patchett, P.J., Jeppsson., L., 2012. U-Pb (zircon) age constraints on the timing and duration of Wenlock (Silurian) paleocommunity collapse and recovery during the "Big Crisis". GSA Bulletin, 124(11/12): 1841 - 1857.

Cramer, B.D., Loydell, D.K., Samtleben, C., Munnecke, A., Kaljo, D., Maennik, P., Martma, T., Jeppsson, L., Kleffner, M.A., Barrick, J.E., Johnson, C.A., Emsbo, P., Joachimski, M., Bickert, T., Saltzman, M.R., 2010. Testing the limits of Paleozoic chronostratigraphic correlation via high-resolution (<500 k.y.) integrated conodont, graptolite, and carbon isotope ($\delta^{13}C_{carb}$) biochemostratigraphy across the Llandovery–Wenlock (Silurian) boundary: Is a unified Phanerozoic time scale achievable? GSA Bulletin, 122(9/10): 1700 - 1716.

Cramer, B.D., Saltzman, M.R., 2005. Sequestration of ^{12}C in the deep ocean during the early Wenlock (Silurian) positive carbon isotope excursion. Palaeogeography Palaeoclimatolofy Palaeoecology, 219: 333 - 349.

Cummins, R.C., Finnegan, S., Fike, D.A., Eiler, J.M., Fischer, W.W., 2014. Carbonate clumped isotope constraints on Silurian ocean temperature and seawater $\delta^{18}O$. Geochim. et Cosmochim. Acta, 140: 241-258.

de La Rocha, C.L., 2003. The Biological Pump. In: Elderfield, H. (Ed.), Treatise on Geochemistry, pp. 83 - 111.

Delabroye, A., Vecoli, M., 2010. The end-Ordovician glaciation and the Hirnantian Stage: A global review and questions about Late Ordovician event stratigraphy. Earth Science Reviews, 98: 269 - 282.

Eiler, J.M., 2007. "Clumped-isotope" geochemistry—The study of naturally-occurring, multiply-substituted isotopologues. Earth and Planetary Science Letters, 262: 309 - 327.

Emiliani, C., Edwards, G., 1953. Tertiary ocean bottom temperatures. Nature, 171: 887-888.

Faerber, C., Munnecke, A., 2014. Gypsum evaporites in a patch reef of the upper Slite Group in the Silurian (Wenlock) of Gotland, Sweden. GFF, 136(1): 75 - 79.

Fike, D.A., Bradley, A.S., Rose, C.V., 2015. Rethinking the Ancient Sulfur Cycle. Annual Review of Earth & Planetary Sciences, 43: 20.1 - 20.30.

Fike, D.A., Finke, N., Zha, J., Blake, G., Hoehler, T.M., Orphan, V.J., 2009. The effect of sulfate concentration on (sub)millimeter-scale sulfide δ34S in hypersaline cyanobacterial mats over the diel cycle. Geochimica et Cosmochimica Acta, 73: 6187 - 6204.

Fike, D.A., Gammon, C.L., Ziebis, W., Orphan, V.J., 2008. Micron-scale mapping of sulfur cycling across the oxycline of a cyanobacterial mat: a paired nanoSIMS and CARD-FISH approach. ISME Journal, 2: 749 - 759.

Fike, D.A., Grotzinger, J.P., 2008. A paired sulfate-pyrite $\delta^{34}S$ approach to understanding the evolution of the Ediacaran-Cambrian sulfur cycle. Geochimica et Cosmochimica Acta, 72(11): 2636 - 2648.

Fike, D.A., Grotzinger, J.P., Pratt, L.M., Summons, R.E., 2006. Oxidation of the Ediacaran Ocean. Nature, 444(7 December 2006): 744 - 747.

Finnegan, S., Bergmann, K., Eiler, J.M., Jones, D.S., Fike, D.A., Eisenman, I., Hughes, N.C., Tripati, A.K., Fischer, W.W., 2011. The magnitude and duration of Late Ordovician-Early Silurian glaciation. Science, 331`: 903 - 906.

Finnegan, S., Fike, D.A., Jones, D.S., Fischer, W.W., 2012. A Temperature-Dependent Positive Feedback on the Magnitude of Carbon Isotope Excursions. Geoscience Canada, 39: 122 - 131.

Fry, B., Ruf, W., Gest, H., Hayes, J.M., 1988. Sulfur isotope effects associated with oxidation of sulfide by O-2 in aqueous solution. Chemical Geology, 73(3): 205-210.

Gao, J., Fike, D.A., Aller, R.C., 2013. Enriched Pyrite δ34S Signals in Modern Tropical Deltaic Muds, AGU 2013 Annual Meeting, San Francisco, CA, pp. B31A-0352.

Garrels, R.M., Lerman, A., 1984. Coupling of the sedimentary sulfur and carbon cycles; an improved model. American Journal of Science, 284(9): 986 - 1007.

Gill, B.C., Lyons, T.W., Saltzman, M.R., 2007. Parallel, high-resolution carbon and sulfur isotope records of the evolving Paleozoic marine sulfur reservoir. Palaeogeography Palaeoclimatology Palaeoecology, 256(3-4): 156-173.

Gill, B.C., Lyons, T.W., Young, S.A., Kaljo, D., Saltzman, M.R., 2014. Sulfur Isotope Evidence for Late Ordovician Ocean Oxygenation: Implications for the Drivers of the Hirnantian Extinction, GSA Annual Meeting. Geological Society of America, Vancouver, British Columbia, pp. 625.

Gill, B.C., Lyons, T.W., Young, S.A., Kump, L.R., Knoll, A.H., Saltzman, M.R., 2011. Geochemical evidence for widespread euxinia in the Later Cambrian ocean. Nature, 469: 80 - 83.

Gomes, M.L., Hurtgen, M.T., 2013. Sulfur isotope systematics of a euxinic, low-sulfate lake: Evaluating the importance of the reservoir effect in modern and ancient oceans. Geology, 41(6): 663 - 666.

Gomes, M.L., Hurtgen, M.T., 2015. Sulfur isotope fractionation in modern euxinic systems: Implications for paleoenvironmental reconstructions of paired sulfate-sulfide isotope record. Geochim. et Cosmochim. Acta, 157: 39 - 55.

Gorjan, P., Kaiho, K., Fike, D.A., Xu, C., 2012. Carbon- and sulfur-isotope geochemistry of the Hirnantian (Late Ordovician) Wangjiawan (Riverside) section, South China: Global correlation and environmental event interpretation. Palaeogeography, Palaeoclimatology, Palaeoecology, 337-338: 14-22.

Grahn, Y., Caputo, M.V., 1992. Early Silurian glaciations in Brazil. Palaeogeography Palaeoclimatolofy Palaeoecology, 99: 9 - 15.

Habicht, K.S., Canfield, D.E., Rethmeier, J., 1998. Sulfur isotope fractionation during bacterial reduction and disproportionation of thiosulfate and sulfite. Geochimica Et Cosmochimica Acta, 62(15): 2585-2595.

Habicht, K.S., Gade, M., Thamdrup, B., Berg, P., Canfield, D.E., 2002. Calibration of Sulfate Levels in the Archean Ocean. Science, 298(5602): 2372-2374.

Hammarlund, E.U., Dahl, T.W., Harper, D.A.T., Bond, D.P.G., Nielsen, A.T., Bjerrum, C.J., Schovsbo, N.H., Schönlaub, H.P., Zalasiewicz, J.A., Canfield, D.E., 2012. A sulfidic driver for the end-Ordovician mass extinction. Earth and Planetary Science Letters, 331-332: 128-139.

Hayes, J.M., 1993. Factors controlling the 13C contents of sedimentary organic compounds: Principles and evidence. Marine Geology, 113(111 - 125).

Hayes, J.M., 2001. Fractionation of carbon and hydrogen isotopes in biosynthetic processes, Stable Isotope Geochemistry. Reviews in Mineralogy & Geochemistry, pp. 225-277.

Hayes, J.M., Strauss, H., Kaufman, A.J., 1999. The abundance of ^{13}C in marine organic matter and isotopic fractionation in the global biogeochemical cycle of carbon during the past 800 Ma. Chemical Geology, 161(1-3): 103-125.

Holser, W.T., 1977. Catastrophic chemical events in the history of the ocean. Nature, 267: 403 - 408.

Holser, W.T., Schidlowski, M., Mackenzie, F.T., Maynard, J.B., 1988. Geochemical cycles of carbon and sulfur. In: Gregor, C.B., Garrels, R.M., MacKenzie, F.T., Maynard, J.B. (Eds.), Chemical cycles in the evolution of the Earth. John Wiley & Sons, New York, pp. 105 - 175.

Hughes, H.E., Ray, D.C., 2016. The carbon isotope and sequence stratigraphic record of the Sheinwoodian and lower Homerian stages (Silurian) of the Midland Platform, UK. Palaeogeography Palaeoclimatolofy Palaeoecology, 445: 997 - 114.

Hughes, H.E., Ray, D.C., Brett, C.E., 2014. $\delta^{13}C_{carb}$ data recording the early Sheinwoodian carbon isotope excursion on the Midland Platform, UK. GFF, 136(1): 110 - 115.

Husson, J.M., Higgins, J.A., Maloof, A.C., Schoene, B., 2015. Ca and Mg isotope constraints on the origin of Earth's deepest $\delta^{13}C$ excursion. Geochimica Et Cosmochimica Acta, 160: 243-266.

Jeppsson, L., 1983. Silurian conodont faunas from Gotland. Fossils and Strata, 15: 121–144.

Jeppsson, L., 1990. An oceanic model for lithological and fauna changes tested on the Silurian record. Journal of the Geological Society, London, 147: 663 - 674.

Jeppsson, L., 1997a. The anatomy of the Mid-Early Silurian Ireviken Event and a scenario for P-S events. In: Brett, C.E., Baird, G.C. (Eds.), Paleontological Events: Stratigraphic, Ecological, and Evolutionary Implications. Columbia University Press, New York, NY, pp. 451 - 492.

Jeppsson, L., 1997b. A new latest Telychian, Sheinwoodian and early Homerian (Early Silurian) standard conodont zonation. Transactions of the Royal Society of Edinburgh, Earth Sciences, 88: 91 - 114.

Jeppsson, L., Eriksson, M.E., Calner, M., 2006. A latest Llandovery to latest Ludlow high-resolution biostratigraphy based on the Silurian of Gotland—a summary. Geol. Foeren. Stockholm Foerh., 128: 109–114.

Jones, D.S., Fike, D.A., 2013. Dynamic sulfur and carbon cycling through the end-Ordovician extinction revealed by paired sulfate-pyrite d34S. Earth and Planetary Science Letters, 363: 144 - 155.

Jones, D.S., Fike, D.A., Finnegan, S., Fischer, W.W., Schrag, D.P., McCay, D., 2011. Terminal Ordovician carbon isotope stratigraphy and glacioeustatic sea-level change across Anticosti Island (Québec, Canada). Geological Society of America Bulletin, 123: 1645 - 1664.

Kaljo, D., Grytsenko, V., Martma, T., Mõtus, M.-A., 2007. Three global carbon isotope shifts in the Silurian of Podolia (Ukraine): stratigraphical implications. Estonian Journal of Earth Sciences, 56: 205 - 220.

Kaljo, D., Kiipli, T., Martma, T., 1997. Carbon isotope event markers through the Wenlock–Přídolí sequence at Ohesaare (Estonia) and Priekule (Latvia). Palaeogeography Palaeoclimatolofy Palaeoecology, 132: 211 - 223.

Kaljo, D., Kiipli, T., Martma, T., 1998. Correlation of carbon isotope events and environmental cyclicity in the East Baltic Silurian. In: Landing, L., Johnson, M.E. (Eds.), Silurian Cycles—Linkages of Dynamic Stratigraphy with Atmospheric, Oceanic, and Tectonic Changes. New York State Museum Bulletin pp. 491: 297 - 312.

Kaljo, D., Martma, T., Männik, P., Viira, V., 2003. Implications of Gondwana glaciations in the Baltic late Ordovician and Silurian and a carbon isotopic test of environmental cyclicity. Bull. Soc. Geol. Fr. , 174: 59.

Kaljo, D., Martma, T., Neuman, B.E.E., Rønning, K., 2004. Carbon isotope dating of several uppermost Ordovician and Silurian sections in the Oslo region., Wogogob Meeting, pp. 51–52.

Kampschulte, A., Strauss, H., 2004. The sulfur isotopic evolution of Phanerozoic seawater based on the analysis of structurally substituted sulfate in carbonates. Chemical Geology, 204(3-4): 255-286.

Kump, L.R., Arthur, M.A., 1999. Interpreting carbon-isotope excursions: carbonates and organic matter. Chemical Geology, 161(1-3): 181-198.

Kump, L.R., Arthur, M.A., Patzkowsky, M., Gibbs, M., Pinkus, D.S., Sheehan, P.M., 1999. A weathering hypothesis for glaciation at high atmospheric pCO_2 during the Late Ordovician. Palaeogeography Palaeoclimatology Palaeoecology, 152: 173 - 187.

Kump, L.R., Garrels, R.M. 1986. Modeling atmospheric O_2 in the global sedimentary redox cycle. American Journal of Science, 286: 337-360.

Laws, E.A., Popp, B.N., Bidigare, R.R., Kennicutt, M.C., Macko, S.A., 1995. Dependence of phytoplankton carbon isotopic composition on growth-rate and $[CO_2](aq)$ - theoretical considerations and experimental results. Geochimica Et Cosmochimica Acta, 59(6): 1131-1138.

Leavitt, W.D., Halevy, I., Bradley, A.S., Johnston, D.T., 2013. Influence of sulfate reduction rates on the Phanerozoic sulfur isotope record. Proceedings of the National Academy of Sciences, 110: 11244 - 11249.

Lehnert, O., Mannik, P., Joachimski, M.M., Calner, M., Fryda, J., 2010. Palaeoclimate perturbations before the Sheinwoodian glaciation: A trigger for extinctions during the 'Ireviken Event'. Palaeogeography Palaeoclimatolofy Palaeoecology, 296: 320 - 331.

Lécuyer, C., Hutzler, A., Amiot, R., Daux, V., Grosheny, D., Otero, O., Martineau, F., Fourel, F., Balter, V., Reynard, B., 2012. Carbon and oxygen isotope fractionations between aragonite and calcite of shells from modern molluscs. Chemical Geology, 332, 92-101.

Li, C., Love, G.D., Lyons, T.W., Fike, D.A., Sessions, A.L., Chu, X., 2010. A New Stratified Redox Model for the Ediacaran Ocean. Science, 328: 80 - 83.

Loydell, D.K., Frýda, J., 2007. Carbon isotope stratigraphy of the upper Telychian and lower Sheinwoodian (Llandovery–Wenlock, Silurian) of the Banwy River section, Wales. Geological Magazine, 144: 1015 - 1019.

Luo, G., Kump, L., Wang, Y., Tong, J., Arthur, M., Yang, H., Huang, J., Yin, H., Xie, S., 2010. Isotopic evidence for an anomalously low oceanic sulfate concentration following end-Permian mass extinction. Earth and Planetary Science Letters, 300, 101-111.

Marenco, P.J., Corsetti, F.A., Hammond, D.E., Kaufman, A.J., Bottjer, D.J., 2008a. Oxidation of pyrite during extraction of carbonate associated sulfate. Chemical Geology, 247(1-2): 124-132.

Marenco, P.J., Corsetti, F.A., Kaufman, A.J., Bottjer, D.J., 2008b. Environmental and diagenetic variations in carbonate associated sulfate: An investigation of CAS in the Lower Triassic of the western USA. Geochimica et Cosmochimica Acta, 72(6): 1570 - 1582.

McFadden, K.A., Huang, J., Chu, X., Jiang, G., Kaufman, A.J., Zhou, C., Yuan, X., Xiao, S., 2008. Pulsed oxidation and biological evolution in the Ediacaran Doushantuo Formation. Proceedings of the National Academy of Sciences, 105(9): 3197-3202.

Melchin, M.J., Mitchell, C.E., Holmden, C.E., Storch, P., 2013. Environmental changes in the Late Ordovician–early Silurian: Review and new insights from black shales and nitrogen isotopes. GSA Bulletin, 125(11/12): 1635 - 1670.

Munnecke, A., Samtleben, C., Bickert, T., 2003. The Ireviken Event in the lower Silurian of Gotland, Sweden - relation to similar Palaeozoic and Proterozoic events. Palaeogeography Palaeoclimatolofy Palaeoecology, 195(99 - 124).

Noble, P., Zimmerman, M.K., Holmden, C., Lenz, A.G., 2005. Early Silurian (Wenlockian) $\delta^{13}C$ profiles from the Cape Phillips Formation, Arctic Canada and their relation to biotic events. Canadian Journal of Earth Sciences, 42: 1419 - 1430.

Opdyke, B.N., Walker, J.C., 1992. Return of the coral reef hypothesis: basin to shelf partitioning of $CaCO_3$ and its effect on atmospheric CO_2. Geology, 20(8): 733 - 736.

Pasquier, V., Sansjofre, P., Rabineau, M., Revillon, S., Houghton, J., Fike, D.A., 2017. Pyrite sulfur isotopes reveal glacial−interglacial environmental changes. PNAS, 114(23): 5941 - 5945.

Paytan, A., Kastner, M., Campbell, D., Thiemens, M.H., 2004. Seawater sulfur isotope fluctuations in the Cretaceous. Science, 304(5677): 1663-1665.

Peng, Y., Bao, H., Pratt, L.M., Kaufman, A.J., Jiang, G., Boyd, D., Wang, Q., Zhou, C., Yuan, X., Xiao, S., Loyd, S., 2014. Widespread contamination of carbonate-associated sulfate by present-day secondary atmospheric sulfate: Evidence from triple oxygen isotopes. Geology, 42(9): 815 - 818.

Present, T.M., Paris, G., Burke, A., Fischer, W.W., Adkins, J.F., 2015. Large Carbonate Associated Sulfate isotopic variability between brachiopods, micrite, and other sedimentary components in Late Ordovician strata. Earth and Planetary Science Letters, 432: 187 - 198.

Raven, M.R., Sessions, A.L., Fischer, W.W., Adkins, J.F., 2016. Sedimentary pyrite $\delta^{34}S$ differs from porewater sulfide in Santa Barbara Basin: proposed role of organic sulfur. Geochim. et Cosmochim. Acta, 186.

Riding, R., Watts, N.R., 1991. The lower Wenlock reef sequence of Gotland: Facies and lithostratigraphy. Geol. Foeren. Stockholm Foerh., 113: 343–372.

Rohrssen, M., Love, G.D., Fischer, W.W., Finnegan, S., Fike, D.A., 2013. Lipid biomarkers record fundamental changes in the microbial community structure of tropical seas during the Late Ordovician Hirnantian glaciation. Geology, 41(2): 127 - 130.

Ruban, D.A., 2008. Silurian biotic crisis in the northern Greater Caucasus (Russia): a comparison with the global record. Palaeontological Research, 12: 387 - 395.

Saltzman, M.R., 2001. Silurian δ13C stratigraphy: a view from North America. Geology, 29: 671 - 674.

Saltzman, M.R., 2005. Phosphorus, nitrogen, and the redox evolution of the Paleozoic oceans. Geology, 33(7): 573-576.

Saltzman, M.R., Thomas, E., 2012. Carbon Isotope Stratigraphy. In: Gradstein, F., Ogg, J., Smith, A. (Ed.), A Geologic Time Scale 2012. Cambridge University Press, Cambridge, U.K., pp. 207 - 232.

Samtleben, C., Munnecke, A., Bickert, T., Pätzold, J., 1996. The Silurian of Gotland (Sweden): facies interpretation based on stable isotopes in brachiopod shells. Geol. Rundsch. , 85: 278–292.

Shackleton, N.J., Opdyke, N.D., 1973. Oxygen isotope and palaeomagnetic stratigraphy of Equatorial Pacific core V28-238: oxygen isotope temperatures and ice volumes on a 10^5 year and 10^6 year scale. Quaternary Research, 3(1): 39 - 55.

Sheehan, P.M., 2001. The Late Ordovician Mass Extinction. Annual Reviews in Earth and Planetary Sciences, 29: 331 - 364.

Sim, M.S., Bosak, T., Ono, S., 2011a. Large Sulfur Isotope Fractionation Does Not Require Disproportionation. Science, 333: 74 - 77.

Sim, M.S., Ono, S., Donovan, K., Templer, S.P., Bosak, T., 2011b. Effect of electron donors on the fractionation of sulfur isotopes by a marine Desulfovibrio sp. Geochimica et Cosmochimica Acta, 75: 4244 - 4259.

Sim, M.S., Ono, S., Hurtgen, M.T., 2015. Sulfur Isotope Evidence for Low and Fluctuating Sulfate Levels in the Late Devonian Ocean and the Potential Link with the Mass Extinction Event. Earth and Planetary Science Letters, 419: 52 - 62.

Swart, P., 2008. Global synchronous changes in the carbon isotopic composition of carbonate sediments unrelated to changes in the global carbon cycle. Proceedings of the Natural Academy of Sciences, 105(37): 13741-13745.

Swart, P., Eberli, G., 2005. The nature of the $\delta^{13}C$ of periplatform sediments: Implications for stratigraphy and the global carbon cycle. Sedimentary Geology, 175: 115-129.

Talent, J.A., Mawson, R., Andrew, A.S., Hamilton, P.J., Whitford, D.J., 1993. Middle Palaeozoic extinction events; faunal and isotopic data. Palaeogeography Palaeoclimatolofy Palaeoecology, 104: 139 - 152.

Tarhan, L., Droser, M., Planavsky, N.J., Johnston, D.T., 2015. Protracted development of bioturbation through the early Palaeozoic Era. Nature Geoscience, 8: 865 - 869.

Tessier, A., Campbell, P.G.C., Bisson, M., 1979. Sequential extraction procedure for the speciation of particulate trace metals. Analytical Chemistry, 51(7): 844-851.

Torsvik, T.H., Smethurst, M.A., Van der Voo, R., Trench, A., Abrahamsen, N., Halvorsen, E., 1992. Baltica. A synopsis of Vendian-Permian palaeomagnetic data and their palaeotectonic implications. Earth Sci. Rev. , 33: 133–152.

Trotter, J.A., Williams, I.S., Barnes, C.R., Mannik, P., Simpson, A., 2016. New conodont $\delta^{18}O$ records of Silurian climate change: Implications for environmental and biological events. Palaeogeography Palaeoclimatolofy Palaeoecology, 443: 34 - 48.

Vecoli, M., Riboulleau, A., Versteegh, G.J.M., 2009. Palynology, organic geochemistry and carbon isotope analysis of a latest Ordovician through Silurian clastic succession from borehole Tt1, Ghadamis Basin, southern Tunisia, North Africa: palaeoenvironmental interpretation. Palaeogeography, Palaeoclimatology, Palaeoecology, 273: 378 - 394.

Watts, N.R., Riding, R., 2000. Growth of rigid high-relief patch reefs, Mid-Silurian, Gotland, Sweden. Sedimentology, 47: 979–994.

Wenzel, B., Joachimski, M.M., 1996. Carbon and oxygen isotopic compositions of Silurian brachiopods (Gotland/Sweden): palaeoceanographic implications. Palaeogeography, Palaeoclimatology, Palaeoecology, 122: 143 - 166.

Wenzel, B., Lecuyer, C., Joachimski, M.M., 2000. Comparing oxygen isotope records of silurian calcite and phosphate - $\delta^{18}O$ compositions of brachiopods and conodonts. Geochim. et Cosmochim. Acta, 64: 1859–1872.

Wenzel, B.C., 1997. Isotopenstratigraphische Untersuchungen an silurischen Abfolgen und deren paläozeanographische Interpretation. Erlanger Geologische Abhandlungen, 129: 1 - 117.

Werne, J.P., Lyons, T.W., 2005. Pathways of diagenetic organic matter sulfurization and sedimentary sulfur cycling revealed through molecular sulfur isotope analysis. Abstracts of Papers of the American Chemical Society, 229: U890-U891.

Werne, J.P., Lyons, T.W., Hollander, D.J., Formolo, M.J., Damste, J.S.S., 2003. Reduced sulfur in euxinic sediments of the Cariaco Basin: sulfur isotope constraints on organic sulfur formation. Chemical Geology, 195(1-4): 159-179.

Wing, B.A., Halevy, I., 2014. Intracellular metabolite levels shape sulfur isotope fractionation during microbial sulfate respiration. Proceedings of the National Academy of Sciences, 111(51): 18116 - 18125.

Wotte, T., Shields-Zhou, G.A., Strauss, H., 2012. Carbonate-associated sulfate: experimental comparisons of common extraction methods and recommendations toward a standart analytical protocol. Chemical Geology, 326: 132-144.

Wu, N., Farquhar, J., Strauss, H., Kim, S.-T., Canfield, D.E., 2010. Evaluating the S-isotope fractionation associated with Phanerozoic pyrite burial. Geochimica et Cosmochimica Acta, 74: 2053 - 2071.

Yan, D., Chen, D., Wang, Q., Wang, J., Wang, Z., 2009. Carbon and sulfur isotopic anomalies across the Ordovician–Silurian boundary on the Yangtze Platform, South China. Palaeogeography Palaeoclimatology Palaeoecology, 297: 32 - 39.

Young, S.A., Saltzman, M.R., Ausich, W.I., Desrochers, A., Kaljo, D., 2010. Did changes in atmospheric CO2 coincide with latest Ordovician glacialinterglacial cycles? Palaeogeography Palaeoclimatolofy Palaeoecology, 296: 376 - 388.

Zhang, T., Shen, Y., Zhan, R., Shen, S., Chen, X., 2009. Large perturbations of the carbon and sulfur cycle associated with the Late Ordovician mass extinction in South China. Geology, 37: 299 - 302.

Zhou, L., Algeo, T.J., Shen, J., Hu, Z., Gong, H., Xie, S., Huang, J., Gao, S., 2015. Changes in oceanic productivity and redox conditions during the Late Ordovician Hirnantian glaciation. Palaeogeography Palaeoclimatolofy Palaeoecology, 420: 223 - 234.

FIGURES AND TABLE CAPTIONS

Fig. 1: Palaeogeography and locations of the early Silurian Ireviken Bioevent (IBE) and/or the Early Sheinwoodian Carbon Isotope Excursion (ESCIE) (after Lehnert et al. 2010). See Table 1 for relevant references.

Fig. 2: Simplified geological map of the study area in Gotland (adapted from Calner (2008)). Locations of measured stratigraphic sections are denoted by red dots.

Fig. 3: Sedimentology of the Lower Visby Fm - Slite Group, Gotland. (a) Prograding nodular limestone and marl alternations of the Lower and Upper Visby Fms, near Högklint (Section G1). (b) Wavy-bedded to nodular argillaceous limestone interbedded with marls transition upward to packestone with brachiopods, bryozoans, crinoids, and stromatoporoids, Upper Visby Fm, near Högklint (G1). (c) A tabulate coral in the Upper Visby Fm, near Högklint (G1). (d) Grainstone within Högklint Fm, Galgberget (G5). (e) Stromatoporoid within the Tofta Fm, Galgberget (G5). (f) Coarse cross-bedded intraclast grainstone with crinoids and brachiopods, Upper Slite Fm, Slite Harbor (G8). (g) Crinoidal grainstone with stylolites within the Upper Slite Fm, Slite Harbor (G8). (h) Intercalated wackestone and green marl with common rugose corals, brachiopods, and trilobites, Slite Fm, near Cementa quarry (G13).

Fig. 4: Composite data, color/symbol coded by section ($\delta^{13}C_{carb}$, $\delta^{18}O_{carb}$, $\delta^{13}C_{org}$, $\delta^{34}S_{SO4}$, $\delta^{34}S_{pyr}$). See Fig. 2 for section locations. Conodont data and zonation showing faunal turnover are from Cramer et al. (2010). The closed circles at the tops of ranges indicate last appearances, with the exception of *Ozarkodina paraconfluens*, which first appears at datum 4 before a disappearance at datum 6. *O. paraconfluens* does return at a higher stratigraphic level on Gotland, as indicated by the arrow above the closed circle at datum 6. Conodont abbreviations: *Pt.—Pterospathodus*; *Ps— Pseudooneotodus*; *p.—pennatus*; *K—Kockelella*; *Pt. am. amorphognath.—Pterospathodus amorphogna- thoides amorphognathoides*.

Fig. 5. Crossplots of phase abundance and isotopic composition. (a) Percent carbonate and $\delta^{13}C_{carb}$. Increasing carbonate content is associated with the onset of elevated $\delta^{13}C_{carb}$ during the Ireviken excursion. (b) TOC (wt %) and $\delta^{13}C_{org}$. Decreased TOC is associated with the elevated $\delta^{13}C_{org}$ during the Ireviken excursion. (c) CAS abundance (ppm) and $\delta^{34}S_{CAS}$. Decreased CAS abundance is associated with the elevated $\delta^{34}S_{CAS}$ during the Ireviken excursion. (d) Pyrite (wt % S) and $\delta^{34}S_{pyr}$. Decreased pyrite abundance is associated with elevated and variable $\delta^{34}S_{pyr}$ during the Ireviken excursion.

Fig. 6: Stratigraphic column and associated data for the G4 section. The strong dependence of the $\delta^{34}S_{pyr}$ signature on lithofacies can be clearly seen.

Table 1. Palaeogeography and locations of the early Silurian Ireviken Bioevent (IBE) and/or the Early Sheinwoodian Carbon Isotope Excursion (ESCIE; after Lehnert et al. (2010)). This table pairs with the map illustrating palaeogeographic reconstruction modified from Cocks & Torsvik (2002) and Lehnert et al. (2010) (Fig. 1). Localities indicate areas where the ESCIE together with facies changes and/or biodiversity changes across the IBE has been recorded. References: Talent et al., 1993; Wenzel & Joachimski, 1996; Jeppsson, 1997b; Kaljo et al., 1997; Wenzel, 1997; Azmy et al., 1998; Kaljo et al., 1998; Saltzman, 2001; Kaljo et al., 2004; Cramer & Saltzman, 2005; Noble et al., 2005; Brand et al., 2006; Kaljo et al., 2007; Loydell & Frýda, 2007; Ruban, 2008; Vecoli et al., 2009; Lehnert et al., 2010; Hughes et al., 2014; Hughes & Ray, 2016.

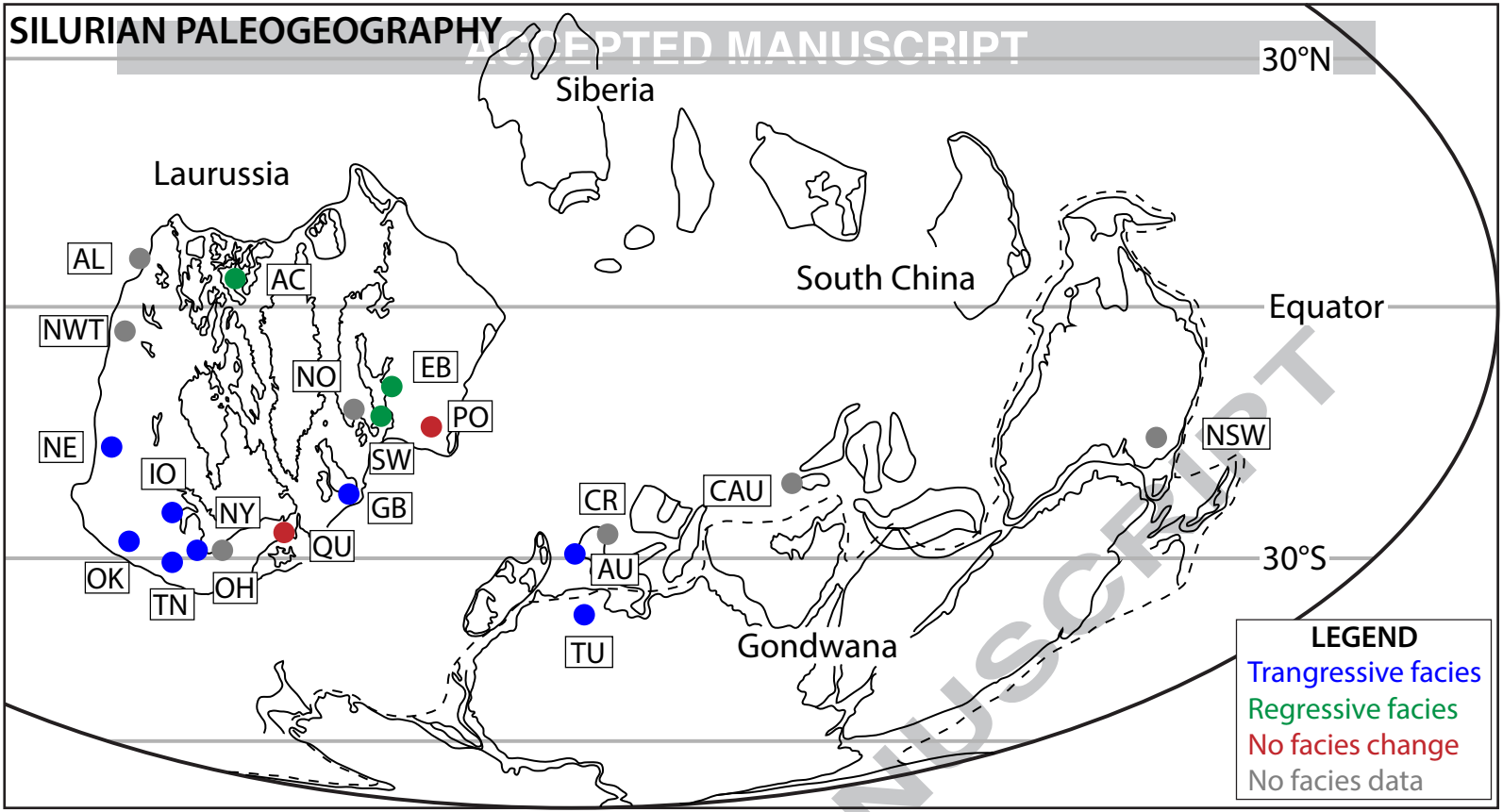
SILURIAN PALEOGEOGRAPHY
ACCEPTED MANUSCRIPT
30°N
Equator
30°S
Siberia
Laurussia
South China
Gondwana
AL
AC
NWT
NO
EB
PO
NE
SW
IO
NY
GB
QU
OK
OH
TN
CR
CAU
AU
TU
NSW
LEGEND
Trangressive facies
Regressive facies
No facies change
No facies data

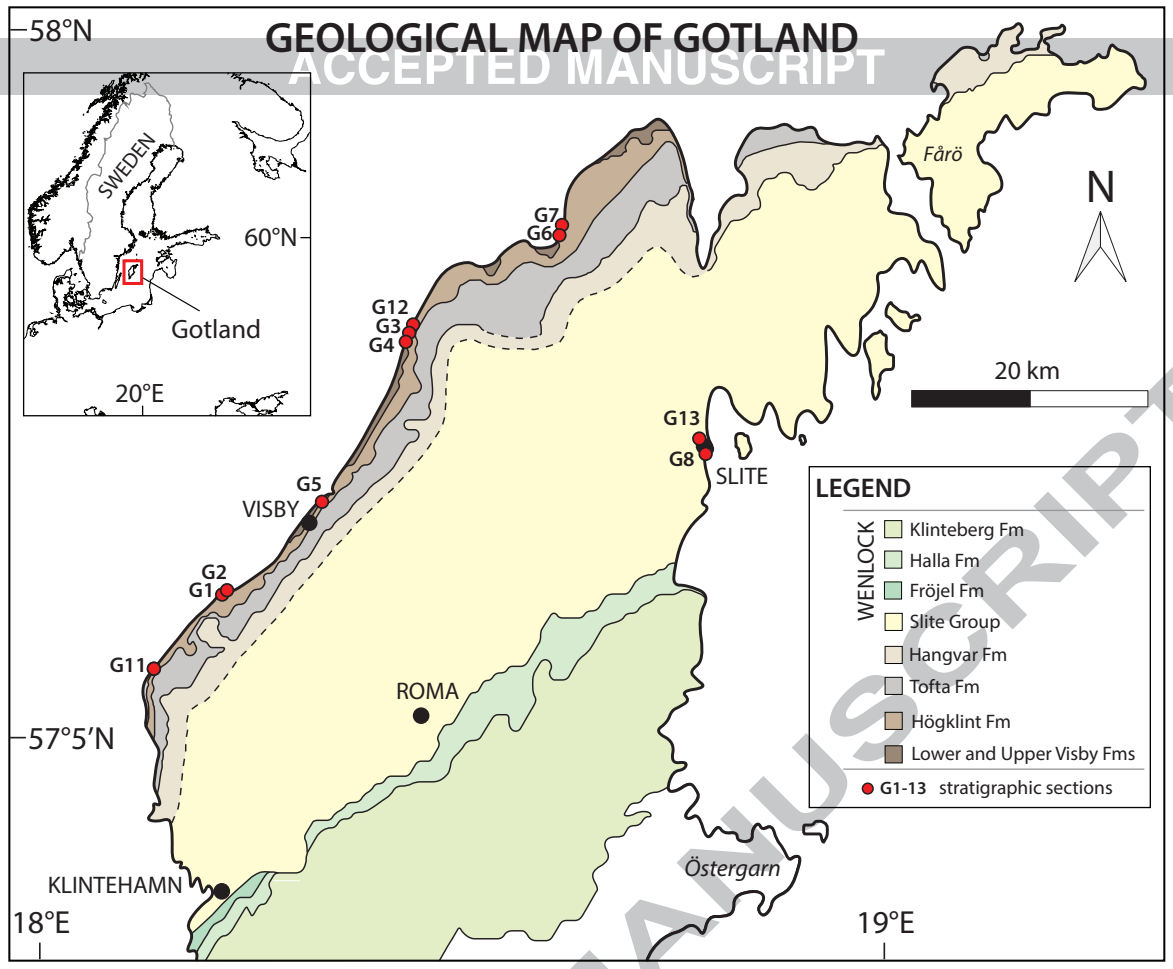

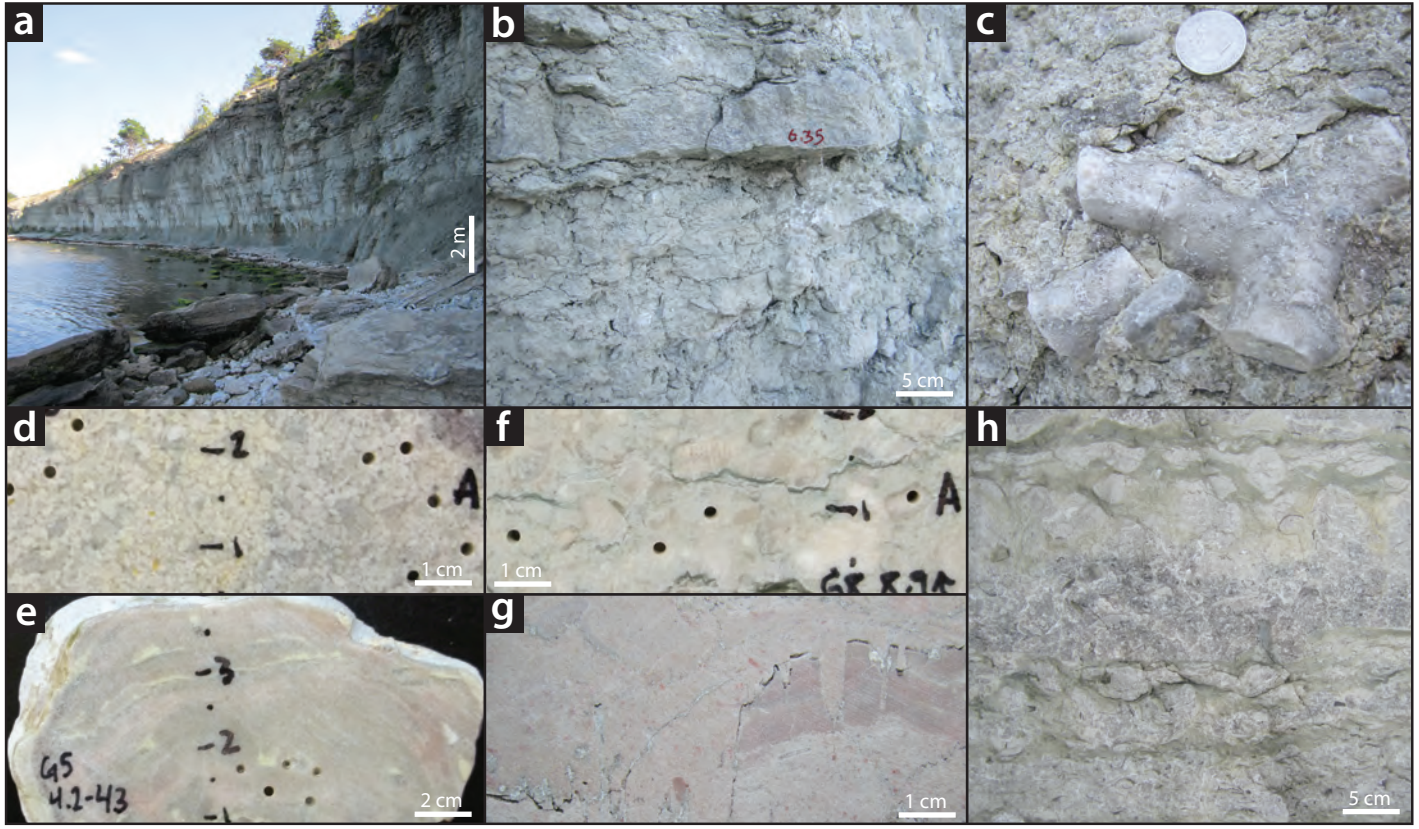
a
2 m
b
635
5 cm
c
d
-2
A
-1
1 cm
f
-1
A
1 cm
h
5 cm
e
-3
-2
GS
4.2-43
-1
2 cm
g
1 cm

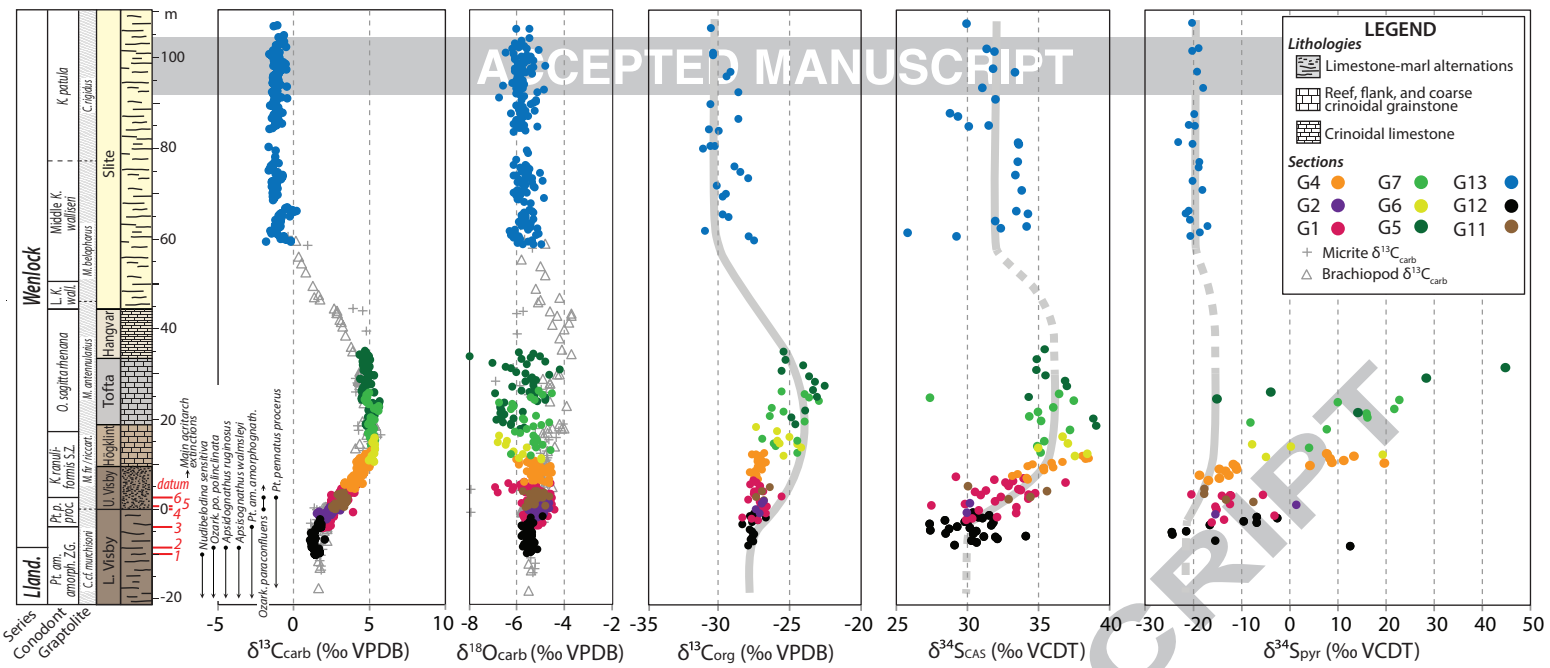

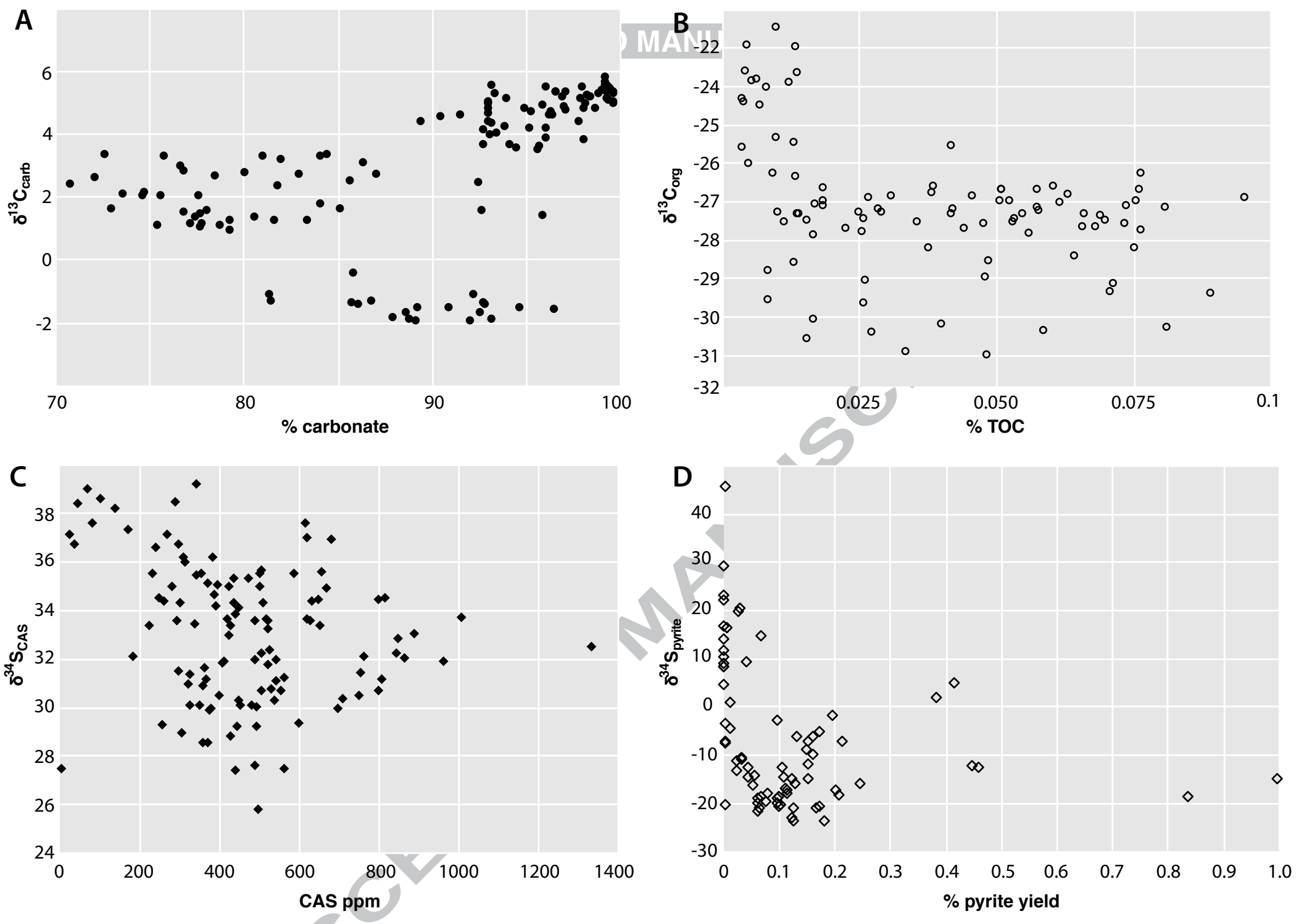
A
$\delta^{13}C_{carb}$
% carbonate
B
$\delta^{13}C_{org}$
% TOC
C
$\delta^{34}S_{CAS}$
CAS ppm
D
$\delta^{34}S_{pyrite}$
% pyrite yield

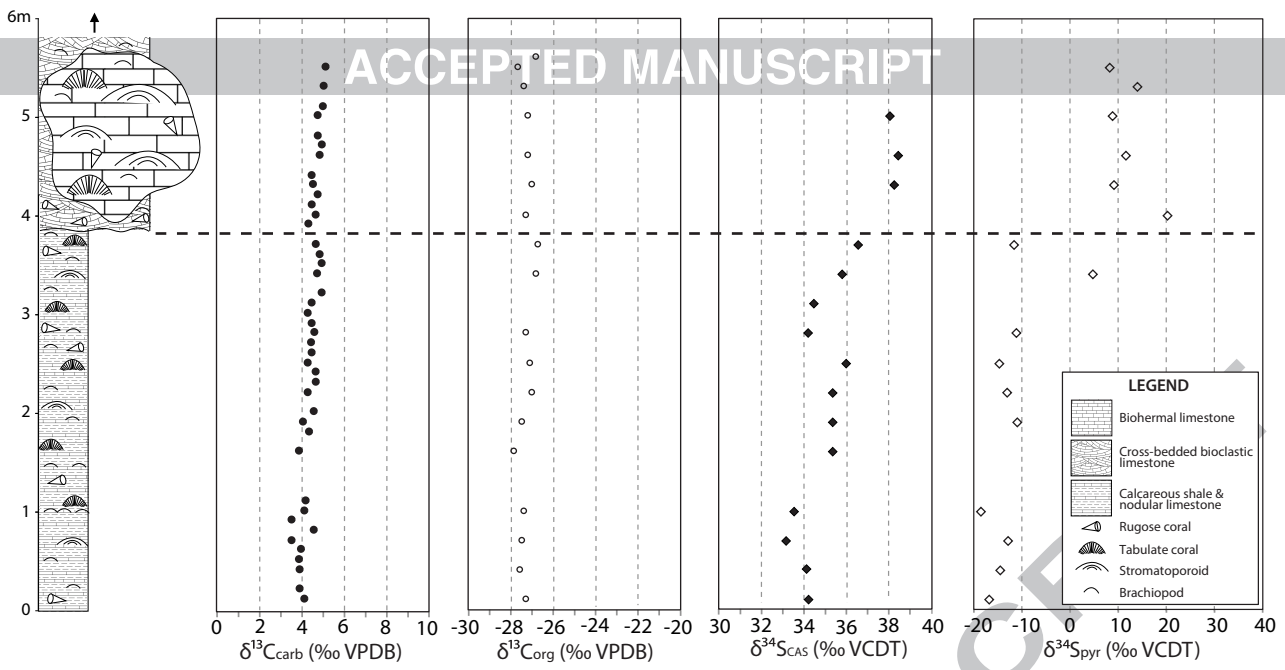

Table 1: Palaeogeography and locations of the early Silurian Ireviken Bioevent (IBE) and/or the Early Sheinwoodian Carbon Isotope Excursion (ESCIE).

Location*	Facies	Data	Magnitude of $\delta^{13}C$ excursion	Reference
Transgressive facies associated with $\delta^{13}C$ excursion				
Tennessee (TN)	Wackestone / packstone with transition to argillaceous interval marking onset of $\delta^{13}C_{carb}$ excursion; also transition in conodonts.	$\delta^{13}C_{carb}$, $\delta^{18}O_{carb}$	$\delta^{13}C_{carb}$ - increase from 2‰ to 4‰	Cramer & Saltzman (2005)
Iowa (IO)	Crinoidal wackestone / packstone with argillaceous unit marking onset of $\delta^{13}C_{carb}$ excursion.	$\delta^{13}C_{carb}$, $\delta^{18}O_{carb}$	$\delta^{13}C_{carb}$ - increase from 1 to 5‰	Cramer & Saltzman (2005)
Ohio (OH)	Wackestone / packstone with onset of $\delta^{13}C_{carb}$ excursion associated with organic rich interval.	$\delta^{13}C_{carb}$, $\delta^{18}O_{carb}$	$\delta^{13}C_{carb}$ - increase from 1 to 3‰	Cramer & Saltzman (2005)
Nevada (NE)	Bedded chert transitions to skeletal wackestone; end of *amorphognathoide* conodonts.	$\delta^{13}C_{carb}$	$\delta^{13}C_{carb}$ - increase from 0 to 3‰	Saltzman (2001)
Oklahoma (OK)	Transition from skeletal wackestone to shale.	$\delta^{13}C_{carb}$	$\delta^{13}C_{carb}$ - increase from -2 to 4‰	Saltzman (2001)
Tunisia (TU)	Broad transition from fine-grained, immature sandstones, siltstones to shaly to silty sediments with marly interbeds.	$\delta^{13}C_{org}$	$\delta^{13}C_{org}$ - increase from -30 to -28‰	Vecoli et al. (2009)
Great Britain (GB)	Transition from bioturbated mudstone to	$\delta^{13}C_{carb}$, $\delta^{13}C_{org}$	$\delta^{13}C_{org}$ - increase from -30 to -26‰	Jeppsson (1997b); Munnecke et al. (2003); Loydell & Frýda (2007);

	laminated hemipeligite.			Hughes, Ray & Brett (2014); Hughes & Ray (2016)
Regressive facies associated with $\delta^{13}C$ excursion				
Arctic Canada (AC)	Transition from platy calcareous shale to interbedded with limestone beds; widespread eustatic low-stand.	$\delta^{13}C_{carb}$, $\delta^{13}C_{org}$	$\delta^{13}C_{carb}$ - increase from 1 to 3‰; $\delta^{13}C_{org}$ - increase from -29.5 to -27‰ but time lag	Noble et al. (2005)
Sweden (SW)	Micrite/wackestone / packstone with subaerial exposures in Hogklint Fm. Heavy $\delta^{13}C_{carb}$ & $\delta^{18}O_{carb}$ values recorded during sea-level lowstands.	$\delta^{13}C_{carb}$, $\delta^{18}O_{carb}$	$\delta^{13}C_{carb}$ - increase from 1 to 4‰;	Wenzel & Joachimski (1996)
East Baltic (EB)	Estonia – onset of $\delta^{13}C_{carb}$ excursion associated with transition from shale to brown marl. Latvia – not onset but peak of $\delta^{13}C_{carb}$ excursion coincides with transition from shale to marl.	$\delta^{13}C_{carb}$, $\delta^{18}O_{carb}$	$\delta^{13}C_{carb}$ - increase from 0 to 4‰; $\delta^{13}C_{carb}$ - increase from 0 to 3‰	Kaljo et al. (1997); Kaljo et al. (1998)
No facies variability associated with $\delta^{13}C$ excursion				
Quebec (QU)	Reefal facies.	Brachiopod $\delta^{13}C_{carb}$, $\delta^{18}O_{carb}$	Subtle relationship with sea-level stands of Johnson et al. (1991) but diagenesis.	Azmy et al. (1998)
Podolia (PO)	Onset of $\delta^{13}C_{carb}$ excursion associated with transition from marl to dolomite. Facies changes but not consistent.	$\delta^{13}C_{carb}$, $\delta^{18}O_{carb}$	$\delta^{13}C_{carb}$ - increase from 0 to 6‰	Kaljo et al. (2007)
No detailed facies and/or isotope data				

Alaska (AL)	—	Conodont morphology	—	Jeppsson (1997b)
North West Territories (NWT)	—	Conodont morphology	—	Jeppsson (1997b)
New York & Ontario (NY)	No facies data but authors suggest that Gotland samples record lighter $\delta^{13}C_{carb}$ values (~ −1.0‰), whilst Estonian samples record heavier $\delta^{13}C_{carb}$ values from a deeper marine setting (Heath et al., 1998; ~ + 2.0‰).	Brachiopod $\delta^{13}C_{carb}$, $\delta^{18}O_{carb}$	$\delta^{13}C_{carb}$ - increase from 1 to 5‰; $\delta^{13}C_{carb}$ - increase from 0 to 2‰	Brand et al. (2006)
Norway (NO)	Unspecified.	$\delta^{13}C_{carb}$	$\delta^{13}C_{carb}$ values depend to some extent on the facies characteristics of the rocks measured	Kaljo et al. (2004)
Prague Basin (CR)	Fine grained siliciclastics transition into limestone.	—		Lehnert et al. 2010
New South Wales (NSW)	No detailed facies observations.	$\delta^{13}C_{carb}$, $\delta^{18}O_{carb}$	$\delta^{13}C_{carb}$ - increase from 1 to 4‰	Talent et al. 1993
Greater Caucasus region (CAU)	Sandstone, siltstone and shales.	—	—	Ruban (2008)

*****This table pairs with map illustrating palaeogeographic reconstruction modified from Cocks and Torsvik (2002) and Lehnert et al. 2010. Localities indicate areas where the ESCIE together with facies changes and/or biodiversity changes across the IBE has been recorded.